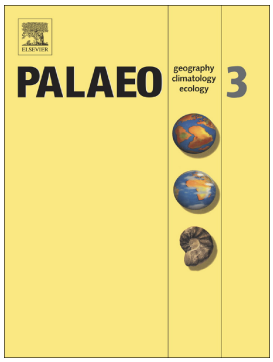

Late Quaternary climatic variability in northern Patagonia, Argentina, based on δ18O of modern and fossil shells of Amiantis purpurata (Bivalvia, Veneridae)

Sol Bayer, Lars Beierlein, Gisela A. Morán, María S. Doldán, Enrique M. Morsan, Thomas Brey, Andreas Mackensen, Laura Farias, Gerardo García, Sandra Gordillo

PII: S0031-0182(20)30457-0

DOI: https://doi.org/10.1016/j.palaeo.2020.110012

Reference: PALAEO 110012

To appear in: *Palaeogeography, Palaeoclimatology, Palaeoecology*

Received date: 3 April 2020

Revised date: 2 September 2020

Accepted date: 3 September 2020

Please cite this article as: S. Bayer, L. Beierlein, G.A. Morán, et al., Late Quaternary climatic variability in northern Patagonia, Argentina, based on δ18O of modern and fossil shells of Amiantis purpurata (Bivalvia, Veneridae), *Palaeogeography, Palaeoclimatology, Palaeoecology* (2019), https://doi.org/10.1016/j.palaeo.2020.110012

Late Quaternary climatic variability in northern Patagonia, Argentina, based on $\delta^{18}O$ of modern and fossil shells of *Amiantis purpurata* (Bivalvia, Veneridae)

Sol Bayer[1,2*], Lars Beierlein[3], Gisela A. Morán[1,4], María S. Doldán[5,6,7], Enrique M. Morsan[6,7], Thomas Brey[3], Andreas Mackensen[3], Laura Farias[8], Gerardo García[8] and Sandra Gordillo[9,10]

[1]Facultad de Ciencias Exactas, Físicas y Naturales, Universidad Nacional de Córdoba.

[2]Centro de investigaciones en Ciencias de la Tierra, (CICTERRA), CONICET and Universidad Nacional de Córdoba, Edificio CICTERRA, Av. Vélez Sársfield 1611, X5016CGA, Ciudad Universitaria, Córdoba, Argentina.

[3]Alfred Wegener Institute, Helmholtz Centre for Polar and Marine Research, Am Handelshafen 12, 27570 Bremerhaven, Germany.

[4] Consejo Nacional de Investigaciones Científicas y Tecnológicas (CONICET), Instituto de Diversidad y Ecología Animal (IDEA). Avda. Vélez Sarsfield 299, X5016GCA. Córdoba, Argentina.

[5]Consejo Nacional de Investigaciones Científicas y Técnicas (CONICET), Buenos Aires, Argentina.

[6]Centro de Investigación Aplicada y Transferencia Tecnológica en Recursos Marinos "Almirante Storni" (CIMAS-CONICET), Güemes 1030, R8520CXV, San Antonio Oeste, Río Negro, Argentina

[7]ESCiMar, Universidad Nacional del Comahue, San Martín 224, San Antonio Oeste, Río Negro, Argentina.

[8]Departamento de Oceanografia, Universidad de Concepción, Centro de Ciencia del Clima y la Resiliencia (CR2), Casilla 2407-10, Concepción, Chile.

[9]Universidad Nacional de Córdoba. Facultad de Filosofía y Humanidades. Museo de Antropología. Córdoba, Argentina.

[10]Consejo Nacional de Investigaciones Científicas y Tecnológicas (CONICET), Instituto de Antropología de Córdoba (IDACOR). Avda. Hipólito Yrigoyen 174, X5000JHO, Córdoba, Argentina.

* sol.bayer@conicet.gov.ar, larsbeierlein@awi.de, gisela.amoran@gmail.com, msdoldan@gmail.com, qmorsan@gmail.com, thomas.brey@awi.de, andreas.mackensen@awi.de, laura.farias@udec.cl, gegarcia@udec.cl, gordillo.sandra@unc.edu.ar

Abstract

Amiantis purpurata is a common warm-temperate water bivalve species distributed from southern Brazil to northern Patagonia, Argentina, which has a rich and well preserved fossil record in the San Matías Gulf (SMG) dating back to the late Quaternary. This study aims to establish *A. purpurata* shells as a new palaeoarchive of past marine conditions in South America. We compared the stable oxygen and carbon profiles ($\delta^{18}O_{shell}$; $\delta^{13}C_{shell}$) of eleven specimens of *A. purpurata* from different geological times (modern, Late Holocene and interglacial Late Pleistocene), and additionally present *in situ* oxygen isotope values of seawater within SMG ($\delta^{18}O_{water}$). Using both sets of information, we calculated and reconstructed palaeowater temperatures for the Late Holocene and compared them to modern water temperatures. Our findings indicate that *A. purpurata* records past environmental parameters such as water temperatures on a seasonal scale and can therefore be considered a suitable candidate for future palaeoenvironmental reconstructions in Northern Patagonia. This study is the first step towards further stable isotope analyses on fossil *A. purpurata* shells, which will show whether and if so, to what extent, important global climate events such as the Neoglacial (Early Holocene), the Hypsithermal (Middle Holocene) and the Little Ice Age (Late Holocene) occurred in South America.

Keywords: oxygen isotopes, seasonality, Holocene, Pleistocene, palaeotemperatures, palaeoarchives

1. Introduction

Knowledge of past climates, in particular the details of palaeoclimatic variability, is crucial to validate well-constrained predictive numerical climate and ecosystem models (Schöne and Gillikin, 2013). Although a variety of palaeoarchives are utilized to improve our knowledge of palaeoclimate and palaeoenvironmental variability, all have spatial and temporal limitations. Carbonate shells of many bivalve species are good archives because they provide temporally high-resolution and well-constrained records of environmental change (Dutton et al., 2002; Hippler et al., 2013). These archives that have been experimentally calibrated provide information on modern and past environmental conditions (Elliot et al., 2009), such as water temperature (Chauvaud et al., 2005; Gillikin et al., 2005; Wanamaker et al., 2006; 2008; Surge and Lohmann, 2008; Aubert et al., 2009), salinity (Klein et al., 1996; Gillikin et al., 2006) or ocean circulation (Carré et al., 2005). This is partially evidenced by the steady stream of special issues on the subject (Schöne and Surge, 2005; Gröcke and Gillikin, 2008; Oschmann, 2009; Wanamaker et al., 2011; Schöne and Gillikin, 2013; Black et al., 2017; Butler and Schöne, 2017; Prendergast et al., 2017, Butler et al., 2019, Gillikin et al., 2019 and that issue). However, only a few studies were performed in the Southern Hemisphere and in South America in particular (Carré et al., 2005; Yan et al., 2012; Gordillo et al., 2011; 2015; Rubo et al., 2018, Aguirre et al., 2019).

Molluscan shell material represents the best preserved and the most abundant fossil fauna in Quaternary marine sediments in Patagonia, Argentina (Feruglio, 1950; Gordillo, 1998), particularly at San Matías Gulf (SMG). The SMG (Fig. 1) is located at the northeastern coast of Patagonia and features several different Quaternary mollusc deposits. Throughout the late Quaternary, regional climate at SMG, as well as sea levels, were subject to various changes (Codignotto et al., 1992; Ponce et al., 2011; Fucks et al., 2012; Isla, 2013). The origin of the gulf itself is related to ancient continental depressions, which were flooded by the ocean (Mouzo et al., 1978; Cavallotto and Violante, 2003; Isla, 2013), date back to at least 12,000 years (Ponce et al., 2011; Isla, 2013). The

SMG, especially San Antonio Bay, provides a rich molluscan fossil record of Pleistocene and Holocene deposits (Feruglio, 1950; Fucks et al., 2005; Gordillo et al., 2014) with the aragonitic shells of the bivalve *Amiantis purpurata* being the most abundant and best-preserved fossil specimens in both deposits (Bayer et al., 2013; 2014). At present, *A. purpurata* lives in high densities in SMG (Morsan, 2003). The occurrence of modern and fossil specimens of the same species at the same location makes the SMG an ideal location for a palaeoenvironmental study.

Several biological aspects of *A. purpurata* have been studied, including the ontogenetic age and shell growth (Morsan, 2003; 2007; Papalardo and Morsan, 2004; Morsan and Orensanz, 2004; Morsan and Kroeck, 2005). Annual growth increments in this species can be identified by alternating dark violet growth ring within the shell carbonate, which correspond to warmer seasons (i.e., summer) and lighter pink growth ring corresponding to colder seasons (i.e., winter) (see Fig. 2). The maximum recorded ontogenetic age of *A. purpurata* is 40 years (Morsan and Orensanz, 2004).

Seasonal and environmental variability can be recorded in a shell by variations in the stable oxygen isotope ($\delta^{18}O$) composition of the shell carbonate. This approach may provide information about the environmental conditions during the time interval of shell growth (Urey et al., 1951; O´Neil et al., 1969; Schöne, 2008). The $\delta^{18}O_{shell}$ values depend on the composition of the seawater ($\delta^{18}O_{water}$) and changes in water temperature. Measurements of carbon isotopes ($\delta^{13}C$) within the shell carbonate, however, are still less well understood but are seen as a potential future proxy, e.g. for productivity (Schöne et al., 2005a; Goman et al., 2008; McConnaughey and Gillikin, 2008; Beirne et al., 2012; Reynolds et al., 2017). Therefore, we report $\delta^{13}C$ data here but do not discuss them in a palaeoenvironmental context.

The main goal of this study is to evaluate whether *A. purpurata* qualifies as a potential new palaeoarchive of past marine conditions in South America. For this purpose, the $\delta^{18}O_{shell}$ values in different geologically dated specimens of *A. purpurata* were compared during time periods in the last 200,000 years.

2. Regional setting

The SMG is the largest gulf in Patagonia, a semiarid to arid climate region with a low rate of precipitation (mean annual land surface precipitation is 275±108 mm, Servicio Meteorológico Nacional 1980-2000), as well as a high evaporation rate with absence of natural freshwater input (Rivas and Beier, 1990). The gulf is a semi-enclosed basin (maximum depth: 180 m in the centre) delimited with a shallow sill in the East (60 m) that limits water exchange with the open sea (Mar Argentino). From spring to fall, an intense thermohaline front divides the water into two masses with different oceanographic conditions: relatively cold and less saline waters –similar to open shelf waters (33.7-33.8 ppm)- occur south of the front, whereas warm and saline waters occur north of the front (34.0-35 ppm; Fernández, 1987; Scasso and Piola, 1988; Gagliardini and Rivas, 2004). The difference in temperature can reach 3°C during the main part of the year. In the water mass placed northern of the front, seawater temperatures range, on average, from 10°C in winter (August) to 18.2°C in summer (January) at depth of 20 m. The average tidal amplitude is 7.62 m (maximum 9.2 m). The bottom sediment is mainly sand near the coastline and is gradually mixed with shell fragments, gravel and mud (Morsan et al., 2010).

2.1 San Antonio Bay

San Antonio Bay is located in the northwestern area of the SMG. It is a tidal delta of ~80 km^2 (40°42', 40°50'S and 64°43', 65°07'W) (Fig. 1), which has been flooded by marine transgressions on several occasions in the geological past (Rutter et al., 1989; Ponce et al., 2011). Waters from the NW and NE coasts at both sides of the bay do not mix. Coastal current are driven by the tides and rotates clockwise oriented by long sandy ridges around the mouth of the bay which restricts water interchange (Lanfredi and Pousa, 1988). Salinity ranges 34-35 ppm during winter; in spring it rises progressively reaching 36 ppm by the end of the summer (Fernandez, 1987).

2.2 Geological background in the SMG

The northern area of the SMG exhibits multiple geomorphological features and littoral deposits assigned to two main Quaternary transgressive episodes, which occurred during the late Pleistocene and Holocene (Angulo et al., 1978; Martínez et al., 2001; Fucks et al., 2012).

The transgressive episode that occurred during the late Pleistocene (MIS 7) formed both the spit bars flanking San Antonio Bay (Fucks et al., 2012): Punta Delgado and Punta Villarino. The following transgressive episode (MIS 5e) reached up to 15 m and covered the spit bars and the littoral ridges in the most internal area of San Antonio Bay (Fucks et al., 2012). The coast was an open sea environment subject to a tidal regime (Fucks et al., 2012). From the early Holocene to the present (MIS 1), the SMG has been protected from the open sea, although it has been affected by low energy tidal currents (Favier Dubois et al., 2009; Favier Dubois and Kokot, 2011; Ponce et al., 2011; Fucks et al., 2012) (Fig. 3).

The fossil assemblages of the San Antonio Bay correspond to three different geological ages. The oldest deposits belong to the Pleistocene MIS5. The beach deposits at 10 m above sea level corresponding to the last interglacial or Pleistocene MIS5e. The last interglacial levels are Holocene (Rutter et al., 1989) and modern beaches. These deposits were extensively studied and described by Angulo et al. (1978), Martínez et al. (2001) and Fucks et al. (2012).

3. Autoecology of *A. purpurata*

Amiantis purpurata is a suspension feeder, which lives burrowed in fine sandy or silty-sandy sediments. It is a euryhaline (>30-35‰) warm-temperate water species, inhabiting the intertidal zone up to 15 m water depth (Morsan, 2007). Its modern distribution extends from Espírito Santo (20°S, Brazil) to the northern SMG (41°C, Argentina) (Carcelles, 1944; Castellanos, 1967; Scarabino, 1977; Morsan and Kroeck, 2005). It is one of the few survivors of the middle-late Miocene faunal turnover, which was characterized by the appearance of new taxa, most of them living now along the Argentinean coast (del Rio, 2000; del Rio et al., 2010). The oldest record of

this species is from the upper Miocene in Uruguay (del Rio and Martínez, 1998; del Rio, 2000; Martínez and del Rio, 2005). Its southernmost known living population is at Punta Villarino (SMG, Fig. 1), where the population occurs in high densities reaching up to 10 kg/m^2 at some sites (Morsan, 2003). *Amiantis purpurata* valves are mineralogically composed of aragonite (Bayer et al., 2013); specimens from the SMG are slow-growing and reportedly live for 40 years (Morsan, 2003; Morsan and Kroeck, 2005).

4. Materials and methods

4.1 Shell collection in the field

All shell collection sites consist of rich mollusc shell deposits. At the field (40°42', 40°50'S and 64°43', 65°07'W), Pleistocene and Holocene deposits present cliffs and exposed low tide sandbars, while modern deposits can be found on beaches. Modern shell specimens were collected by hand and taken from the intertidal zone (modern beach) during low tide in summer (Site 1 in Fig. 1; Fig. 4F-G; Table 1). The same sampling method has been conducted for Holocene beach ridges (or sandbars) (Sites 2-4 in Fig. 1; Fig. 4E; Table 1), while volumetric samples (approximately 100 cm^3) were taken from all cliff deposits (Holocene and Pleistocene) (Sites 5-11 in Fig. 1; Fig. 4-D; Table 1). Four shells from the Pleistocene and six shells from the Holocene deposits were selected (cf., Table 1 for details). In addition, one modern shell specimen (with ligament) has been selected from Site 1 (Fig. 1; Table 1). After collection in the field, shells were washed with tap water and stored at the CICTERRA repository (CEGH-UNC).

4.2 Shell preparation

Shell cross-sections were prepared at CIMAS (Centro de Investigación Aplicada y Transferencia Tecnológica en Recursos Marinos "Almirante Storni") in San Antonio Oeste. Shells were cut perpendicular to the growth lines and along the axis of maximum growth from the umbo to the ventral margin using a low-speed precision saw and a 0.4 mm thick diamond-coated saw blade

StruersMinitom (1997). The sections were ground and polished using sandpaper of very fine grain (4000 grit, grain size: 5 μm) on a rotating platform at variable speeds. Cross-sections were prepared following the technique described in Morsan and Orensanz (2004) for *A. purpurata* shells.

4.3 Shell dating

Radiocarbon dates were measured for shell material from sites with appropriate ages for this method. After carefully mechanically removing the periostracum and any adhering sediment from the outer surface of the shells using ultrasonic and a hand drill device (Type Proxxon Minimot 40/E), shells were radiocarbon dated by Liquid Scintillation Spectrometry (LSS) at Laboratorio de Tritio y Radiocarbono (LATyR) in Argentina or by Accelerator Mass Spectrometry (AMS) ^{14}C at the Poznań lab in Poland (cf., Table 1 for details). Calibrated ^{14}C ages (cal. yr B.P.) were calculated using Calib version 7.04 (Stuiver et al., 2020) based on the Marine13 radiocarbon calibration curve (Reimer et al., 2013) and a regional San Matías Gulf (Holocene) marine reservoir effect of ΔR = 266±51 yr (Favier Dubois, 2009). Pleistocene shell material has been dated based on the associated deposit/outcrop, which means that the deposits here were dated by Electro Spin Resonance (ESR) after Rutter et al. (1990) (Table 1).

4.4 Shell preservation – Confocal Raman Microscopy

All fossil and modern shell specimens were checked for traces of recrystallization, i.e., if the pristine aragonite shell has been preserved (Beierlein et al., 2015a; von Leesen et al., 2017). This was achieved by using a confocal Raman microscope (CRM; WITec alpha 300 R; cf., Nehrke et al., 2012), which was equipped with a diode laser (excitation wavelength 488 nm) and a 20× Zeiss objective. Instrumental settings and procedure follow Nehrke et al. (2012). All shells chosen for stable oxygen isotope analysis were checked either by CRM scans or single spot measurements.

4.5 Micro-milling and stable isotope analysis ($\delta^{18}O_{shell}$ and $\delta^{13}C_{shell}$) in shell carbonate

Stable isotope analysis was carried out on each of the eleven *A. purpurata* shells described in this study. Due to growth increments become narrower towards the ventral margin of the shell, only the first four to five ontogenetic years were clearly visually distinguishable in shell specimens (Crippa et al., 2016). In some of the specimens, however, up to eight or nine ontogenetic years were distinguishable (e.g. specimens H362 or H613). Isotope sampling was conducted only in shell areas where a clear distinction of annual growth lines was possible. It is an often observed effect that growth lines in fossil shells are difficult to observe. This is mainly due to decaying organics in the darker organic-rich growth lines (cf., Schöne et al., 2005b; Beierlein et al., 2015a). For the same reason, we could not reliably assign ontogenetic years to the increments in our Pleistocene shells and isotope data. In order to obtain samples of calcium carbonate powder at high spatial resolution, each shell cross-section was sampled using the milling technique (Dettman and Lohmann, 1995). Consecutive samples were taken from the outer shell layer using a 700 µm mill bit (Komet/Gebr. Brasseler GmbH & Co. KG), which was mounted onto an industrial highprecision drill (Minimo C121; Minitor Co., Ltd) and attached to a binocular microscope. Samples were taken parallel to the growth rings (Fig. 2). Each of the samples yielded 15 to 60 µg of carbonate powder.

Isotope ratio mass spectrometry (IRMS) was performed at the Alfred Wegener Institute for Polar and Marine Research (Bremerhaven, Germany) using a Thermo Finnigan MAT 253 coupled with an automated carbonate preparation device (Kiel IV). Measurements were calibrated against an internal NBS-19 laboratory standard (SHKBr2; $\delta^{18}O$ = -4.28‰ and $\delta^{13}C$ = -2.88‰). Results were reported in δ-notation and given as parts per mil (‰ VPDB). The long-term precision (1σ) based on an internal laboratory standard (SHKBr2) measured over a 1-year period together with samples was better than ±0.08‰.

Because ice volume has changed over geological time and therefore has affected marine $\delta^{18}O_{SW}$ values, it was necessary to correct $\delta^{18}O_{shell}$ values with individual factors (based on their specific radiocarbon ages) for each of the Holocene *A. purpurata* specimens by a maximum of

0.02‰. Based on the work of Fairbanks (1989) and following Beierlein et al. (2015b) this allows for comparability between fossil and modern $\delta^{18}O_{shell}$ derived measurements.

4.5.1 Absolute palaeowater temperatures

The reconstruction of palaeowater temperatures from fossil shell material can only be undertaken when considering a number of particularities (i.e., ice volume effect over geological time scales (cf., Section 4.5), knowledge about the water chemistry ($\delta^{18}O_{SW}$; cf., Section 4.6) preservation of shell material (cf., Section 4.2) and taking great care with the interpretation of such results. After careful consideration of the above-mentioned, palaeotemperatures were calculated using the palaeothermometry equation by Grossman and Ku (1986) with a PDB-SMOW scale correction of -0.27‰ (Dettman et al., 1999).

We considered it highly unlikely that we could find a good estimation for a Pleistocene $\delta^{18}O_{SW}$ value. Therefore, no absolute water temperatures for such samples are presented. However, in order to compare seasonality signals recorded in each shell ($\Delta\delta^{18}O$), we calculated the difference between the maximum ($\delta^{18}O_{shell\ max}$) and minimum ($\delta^{18}O_{shell\ min}$) oxygen isotope values consistent with the approach of Wanamaker et al. (2011).

4.6 Stable oxygen isotope analysis in water samples ($\delta^{18}O_{sw}$)

To estimate water temperatures based on the shell carbonate ($\delta^{18}O_{shell}$) it is essential to know about the water chemistry ($\delta^{18}O_{sw}$) of the water the shell grew in. To our knowledge, no measured $\delta^{18}O_{sw}$ values have been published for the SMG so far and can only be inferred from gridded data sets (cf., Section 4.7.2). Therefore, divers collected bottom water samples at Punta Villarino, NW of SMG (40º51´S, 64º44.5´W, star symbol in Fig. 1) in summer, early autumn and winter of 2017. Water samples (500 ml) were filtered with a ϕ 20-25 µm monofilament polyester mesh, closed hermetically and stored in dark for a few months. The $\delta^{18}O_{SW}$ values were determined from 15 ml at the Biogeochemistry Laboratory of the Universidad de Concepción, Chile (Pizarro ®

Analyzer L2130-i, Vaporizer A0211 and Autosampler ALSG). Calibration and optimization of the instrument is performed following van Gelden and Barth (2012). For calibration, three international standards are analysed by quintupled and 10 times per vial (VSMOW 2, SLAP, GIPS) in order to construct a calibration curve. Daily and while the equipment is in use, calibrations are carried out with secondary or internal standards, for this three is a stock of natural waters of different origins with known isotopic composition values. Correction of raw data for analytical effects (i.e., memory and drift) is done according to PICARRO manual by a linear best-fit equation between the known calibration values and the analyser's reported values. Finally, an average was calculated $\delta^{18}O_{SW}$ in order to use it in the palaeothermometry equation.

4.7 Environmental data

The shallow water masses of the SMG show a maximum sea surface temperature of 21˚C in January (summer) and the lowest temperatures of 7.8˚C in July (winter) (Morsan and Kroeck, 2005; Rivas 2010) (Fig. 4). Moreover, the waters of the northwestern area of the SMG present a maximum salinity of 34.15 (Scasso and Piola, 1988; Rivas and Beier, 1990; Gagliardini and Rivas, 2004; Lucas et al., 2005). Additionally, the modern configuration of the gulf restricts the exchange of its waters to the open sea. The mean sea surface temperature is high since it is minimally exposed to the effects of the cold Malvinas Current (Rivas, 2010), and heat transferred from the atmosphere is more efficiently used by shelf waters to increase their sea surface temperature (Krepper and Bianchi, 1982; Scasso and Piola, 1988; Rivas, 1990; Rivas and Pisoni, 2010).

4.7.1 In situ *water temperature measurements*

In order to obtain *in situ* water temperature measurements from the northern area of SMG, average daily water temperature was recorded *in situ* in the water column at El Sótano (40°57.3´S, 65°6.5´W), Northern SMG (7 April 2016 through 28 April 2017) (Fig. 1). The data logger

(OpticStowAway-Tidbit (°C) OnSet ± 0.20°C) was set to six-hour intervals and fixed to a submerged anchor at 4-13 m depths, depending on the seawater level.

5. Results

5.1 Shell dating

Radiocarbon dates were performed with two different dating techniques according to what was available: Liquid Scintillation Spectrometry (LSS) and Accelerator Mass Spectrometry (AMS). The studied shells corresponded all to Late Holocene and one from modern times, less than 3900 years old (Table 1). In addition, we also analysed shells from Late Pleistocene outcrops. Different species of bivalves from these deposits have been dated by ESR (Rutter et al., 1990) (Section 4.3, Table 1).

5.2 Shell preservation – Confocal Raman Microscopy

By means of the Raman microscopy, we were able to identify the mineral composition of the *A. purpurata* shells studied. The Raman spectra showed the characteristic peaks of aragonite (around 206 cm^{-1} and 1085 cm^{-1}, Fig. 5) but no peaks for other carbonate types; i.e., shells were composed of the original aragonite of the shells only without any sign of re-crystallization of calcium carbonate induced by early diagenesis.

5.3 Stable oxygen isotope analysis ($\delta^{18}O_{shell}$ and $\delta^{13}C_{shell}$) in shell carbonate

The $\delta^{18}O_{shell}$ profiles from all shells show a saw-tooth shape (Fig. 6). This oscillating pattern is clearly visible in most of the ontogenetic years sampled but has a different range of amplitude and periodicity, depending also on the specific sampling resolution (per year and in total), the number of ontogenetic years sampled and the stable isotope ratio of the shell carbonate in each of the shells analysed (Table 1). The modern shell, M726, shows a $\delta^{18}O_{shell}$ value range from -

1.10‰ to +0.86‰. The Holocene shells amplitudes vary from -0.64‰ to +1.41‰, while the Pleistocene $\delta^{18}O_{shell}$ values range from -1.99‰ to +1.12‰ (Fig. 7) (Table 1, column 7).

The $\delta^{18}O_{shell}$ oscillations coincide with the seasonal banding pattern of the shell, where the highest values of $\delta^{18}O_{shell}$ correspond to light rings or winter rings, while the lowest values of $\delta^{18}O_{shell}$ correspond to dark rings or summer rings. The seasonal amplitudes differ by geological age (ANOVA $p < 0.0001$; $F = 9.79$).

The intra-annual range of $\delta^{18}O$ ($\Delta\delta^{18}O$) is quite variable among all shells, with the widest delta observed in a Pleistocene shell (P1143) ($\Delta\delta^{18}O_{P1143}$ = 2.26‰), followed by the modern shell (M726) ($\Delta\delta^{18}O_{M726}$ = 1.96‰) and a Holocene shell (H311) ($\Delta\delta^{18}O_{H311}$ = 1.93‰) (Table 1, column 9). The Holocene shell H613 shows the lowest seasonality ($\Delta\delta^{18}O_{H613}$ = 1.25‰) (Table 1, column 9).

The $\delta^{13}C$ profiles show a smoothed oscillating pattern. The modern shell M726 shows a $\delta^{13}C$ value range from -6.34‰ to +1.80‰. Minimum and maximum $\delta^{13}C$ values are -1.18‰ and +3.19‰ in Holocene shells, and -3.59‰ to +2.28‰ in Pleistocene shells (Figs. 6 and 7) (Table 1, column 8).

The intra-annual range values of $\delta^{13}C$ ($\Delta\delta^{13}C$) are variable among all shells, where the widest delta is observed also in the Pleistocene shell P1143 ($\Delta\delta^{13}C_{P1143}$ = 3.39‰), followed by another Pleistocene shell (P1204) ($\Delta\delta^{13}C_{P1204}$ = 2.92‰) (Table 1, column 10). Again, the Holocene shell H613 shows the lowest intra-annual delta values of $\delta^{13}C$ of the Quaternary ($\Delta\delta^{13}C_{H613}$ = 0.23‰) (Table 1, column 10).

5.4 Stable oxygen isotope analysis ($\delta^{18}O_{sw}$) in water samples

The $\delta^{18}O_{sw}$ values (vs. VSMOW) of the bottom water samples from Punta Villarino (40º51´S, 64º44.5´W, star symbol in figure 1) varied between +0.23‰ and +0.27‰ with a mean value of +0.25‰. The water sample taken on summer (February) gave a value of $\delta^{18}O_{sw}$ = +0.27‰,

the one taken on early autumn (March) gave a value of $\delta^{18}O_{sw}$ = +0.23‰, and the sample taken on winter (August) gave a value of $\delta^{18}O_{sw}$ = +0.24‰. These values are the first measurements of $\delta^{18}O_{sw}$ from bottom waters of the San Matias Gulf, NW Patagonia Argentina.

5.5 Water chemistry data ($\delta^{18}O_{sw}$) by the global gridded data set

We obtained seawater $\delta^{18}O_{sw}$ data from the global gridded data set of LeGrande and Schmidt (2006) by using the software Panoply v.4.2.0 (Schumunk, 2017) in order to evaluate the precision of the values obtained by both methods: *in situ* water sampling (Section 4.6; $\delta^{18}O_{sw}$ = +0.25‰) and using software Panoply (Section 4.7.2). The global gridded data set shows that the regional $\delta^{18}O_{sw}$/salinity slope is -0.4‰ psu−1, see also the corresponding NASA website (http://data.giss.nasa.gov/o18data; Schmidt et al., 1999). This value should be taken as hypothetical since SMG has special water dynamics (Section 2). Moreover, there are no actual measurements published before for this area of Patagonia Argentina.

5.6 Absolute palaeowater temperatures

Water temperatures inferred from $\delta^{18}O_{shell}$ differ significantly between Holocene and Modern times (ANOVA $p < 0.0001$; $F = 9.556$). Tukey´s pairwise comparisons showed that Modern reconstructed palaeotemperature variance was significantly different from the Holocene ones except for H688 (2346-2092 yr B.P.). However, shell H688 showed differences with H438 (2351-2182 yr B.P.; $p = 0.017$) and H362 (2286-2134 yr B.P.; $p = 0.001$) (Fig. 8). These comparisons are only valid if the oxygen isotopic composition of seawater remained (relatively) unchanged.

In order to compare seasonality signals recorded in each shell from the late Quaternary ($\Delta\delta^{18}O_{shell}$), we calculated the difference between the maximum ($\delta^{18}O_{shell\ max}$) and minimum ($\delta^{18}O_{shell\ min}$) oxygen isotope values (Table 1).

5.7 In situ *water temperature measurements*

Average monthly water temperature was recorded *in situ* in the water column at Northern SMG (40°57.3´S, 65°6.5´W) from early April (2016) through late April (2017) (Fig. 9). Seawater temperature described an annual cycle with a minimum value of 10.3°C registered at the end of July and a maximum value of 21.1°C registered on late February.

6. Discussion

The main aim of this study is to establish whether *A. purpurata* qualifies as a reliable new palaeoarchive of past (Holocene) marine conditions in South America. For this purpose, a total of eleven shell specimens from different geological times (covering the Pleistocene to modern times) were geochemically ($\delta^{18}O_{shell}$) analysed if seasonal environmental signals are preserved within the shell carbonate of this species. The seasonal colouration pattern within the shell carbonate, the reconstruction of past water temperatures from the shell carbonate as well as future applications for *A. purpurata* shells are discussed below. However, we will refrain from discussing the carbon isotope profiles/data ($\delta^{13}C_{shell}$), as carbon isotopes in bivalve shell carbonates are hardly understood and have not been calibrated successfully in any species so far.

6.1. Seasonal periodicities within modern and fossil shell carbonates of A. purpurata

As observed by Morsan and Orensanz (2004), the external part of the shell of the modern specimen (M726) showed an alternation of dark purple and light pink bands. By using thin- and cross-sections of the modern specimen, an alternation of dark and light bands within the shell carbonate can be observed. Morsan and Orensanz (2004) concluded that these external growth rings corresponded with the internal banding and that external and internal patterns matched in their periodicity. Our $\delta^{18}O_{shell}$ profiles prove that the periodicity is annual and corresponds to the seasonal variations in water temperature at the SMG (Morsan and Orensanz, 2004). In this study, we also show that also the oxygen isotope profile of the modern specimen (M726) exhibits a well-defined

oscillation pattern (cf., Fig. 6). Here, highest values of $\delta^{18}O_{shell}$ correspond to light rings and lowest values to dark rings. We therefore, conclude that in *A. purpurata* the light rings correspond to winter rings and dark rings to summer rings. Assessment of accretion frequencies is a required step in age and growth studies (Beamish and McFarlane, 1983; Campana, 2001). This finding is of utmost importance when studying the fossil shells in which shell colouration (which is usually bound to organics within the shell carbonate) is not preserved. Purple and pink rings on the outside of the shell are no longer visible in fossil shells. Instead, the dark and light rings seen in thin- and cross-sections helped to distinguish between summer and winter (carbonate) portions of the shell.

Moreover, all ten fossil *A. purpurata* shells (Holocene and Pleistocene) showed a periodic cyclicity in their $\delta^{18}O_{shell}$ profiles (Figs. 6 and 7). Highest values of $\delta^{18}O_{shell}$ correspond to light rings whereas lowest values correspond to dark rings within the shell carbonate. We therefore conclude that a seasonal environmental signal is preserved within the fossil *A. purpurata* shells from SMG.

6.2. Modern water temperatures and $\delta^{18}O_{shell}$ profiles of A. purpurata

The NW coast of the SMG is not directly exposed to the cold Malvinas Current, and therefore, the mean SST (15°C) is distinguishably higher than the SST of the open ocean (Rivas, 2010). In a nine-year observational study by Morsan and Kroeck (2005), a clear and pronounced seasonal cyclicity in SST was observed for the NW coast of the SMG. Maximum water temperatures of 22.5°C were recorded in mid-summer (January) while, minimum water temperatures of 6.0°C were recorded in mid-winter (August). *In situ* measurements using a data logger at the study area for the time from early April 2016 to late April 2017, measured in this study, showed that bottom water temperatures vary between 9.5 and 21.0°C (Section 5.7; Fig. 9) giving an amplitude of 11.5°C.

In comparison, the reconstructed water temperature amplitude from the modern *A. purpurata* shell (9°C) was smaller than the one measured *in situ* by the data logger. Furthermore, reconstructed minimum (16°C) and maximum (25°C) water temperatures both were considerably

higher (Fig. 8). Considering the comparison of modern water temperatures (shell vs. water) as well as the reconstruction based on fossil shells there is a list of issues which might play a role and have to be taken into consideration: (1) it is possible, based on the available data so far, that the $\delta^{18}O_{shell}$ values are slightly off equilibrium precipitation, however, given the uncertainties we cannot fully exclude the possibility that it is in equilibrium precipitation with the surrounding water. Physiology is a factor that controls the mode of how environmental changes are recorded in the shell (Schöne, 2008). Chemical composition of the carbonate secreting fluid is modified by metabolic processes and thus, the biogenic hard tissues. Although this has been observed in some bivalve species (e.g., Epstein et al., 1953; Crippa et al., 2016; Rubo et al., 2018) it does not necessarily exclude *A. purpurata* from being a suitable palaeoarchive in the future (Wickson et al., 1999; Gordillo et al., 2015). (2) Due to very limited data, seasonal variations in salinity, which have to be expected, could not be considered when calculating water temperatures from shell carbonate. One average value, based on our *in situ* measurements (Section 5.4) has been calculated and used for all $\delta^{18}O_{shell}$ values. It has to be expected that there is a certain variability by this. (3) The *in situ* bottom water temperatures cover a one-year period (Fig. 9) and due to the unknown precise date of death in the modern shell (M726) we cannot say if the time periods compared here coincide. Also, the location of the *in situ* water measurements might not precisely represent the exact place the modern shell specimen lived in and it might therefore have experienced a slightly different temperature range. (4) Calcium carbonate of the shells precipitates at higher rates during spring and summer. A consistent sampling like the one we applied here (milling, cf., Section 4.5) will have the effect that every shell sample taken will represent a slightly different time interval (ranging approximately from days (fast shell growth) to maybe even months (slow shell growth). Therefore, summer temperatures might be over-represented, while the thinner shell portion precipitated in winter (thin white rings, Fig. 2) is relatively under-represented in the data. Following from this it should be stated that samples representing summer values might have a much higher resolution (e.g., daily) than monthly (to which they are compared) and which might explain the higher summer values observed. If daily

increments in *A. purpurata* were continuously visible throughout the inner shell growth pattern it would be possible to correct for this temporal shift (e.g., by following the method describe in Schöne et al. (2005c) for *Arctica islandica*). Unfortunately, this is to date and with the methods available not possible yet. (5) The elevated minimum values within *A. purpurata* might very likely be explained by the fact that many shells do not precipitate shell carbonate throughout the entire year. In autumn or winter many bivalve species stop their growth e.g., due to reproduction, food availability or cold temperatures. This has also been reported for other species within the SMG, such as *Panopea abbreviata* and *Ostrea puelchana* (Morsan et al., 2012; Boldan et al., 2018).

Finally, it is important to mention that an *in situ* $\delta^{18}O_{sw}$ value for the SMG was of great significance since this gulf has its own special water dynamic, which differs from the open ocean (cf., Section 2) and shows little variation throughout the year. Such a value ($\delta^{18}O_{sw}$) had not been reported before and therefore a reconstruction using stable oxygen isotopes ($\delta^{18}O_{shell}$) would have relied on an interpolated value derived from the global gridded data set (cf., Section 5.5), which in this example and location would have led to very differing values and results. Future studies should take this into consideration and try to measure values over a longer time period (i.e., an entire year) at the exact location the corresponding mollusc population was located.

6.3. Palaeowater temperatures

Palaeotemperature values calculated from Late Holocene shells showed great variability within this geological period (Section 5.6, Fig. 8). Assuming that the seawater oxygen isotope composition has remained constant or with minor change over the Late Holocene, it was possible to estimate seawater temperatures for the period 4000-400 yr B.P. (Fig. 8). The $\delta^{18}O_{shell}$ profiles of the Late Holocene shells resemble the cyclic pattern found in the modern shell but correspond to different temperature ranges, i.e., maximum and minimum temperatures recorded by the shells differ between epochs (Fig. 8). In general, calculated temperatures for the Late Holocene showed significant differences when compared to the modern shell, which showed lower mean temperatures

when compared to the modern shell (~18-19°C and ~21°C, respectively). Even if those values coincide with the cooler temperature pulses interpreted by other authors in Patagonia during the Late Holocene (Schäbitz, 1994; Villalba, 1994; Meyer and Wagner, 2008; Boretto et al., 2013; Strelin et al., 2014) we would be very careful to derive such an interpretation from single shell specimens each representing a slice of a few years, within an interval of a few hundred years. It however very much justifies future studies focussing in more detail at specific time intervals in the past using *A. purpurata* as an archive. When looking at a single specimen, representing an entire time interval within the Holocene it should also be mentioned that, to some degree, the observed differences could also be due to differences in the microhabitat (Hallman et al., 2008). This is due to the fact that the SMG is characterized by a complex geomorphology and water dynamics, which also changed during the Late Holocene (cf., Section 2.2).

The reconstruction of palaeowater temperatures is subject to a list of assumptions and limitations, which have, prior to such a calculation, to be evaluated very carefully (cf., list of issues above). In lack of a robust and trustworthy $\delta^{18}O_{SW}$ value for that time period we did not calculate absolute water temperatures for the Pleistocene specimens. However, it is worth noting that $\delta^{18}O_{shell}$ profiles of the Pleistocene shells also showed a similar cyclic pattern (Fig. 7), as observed in the modern and the Late Holocene shells. The Pleistocene shell P1143 showed the widest intra-annual range observed in the late Pleistocene as well as in the late Quaternary of the study area ($\Delta\delta^{18}O_{P1143}$ = 2.26‰). We therefore conclude, that the late Pleistocene shells showed a pronounced seasonality pattern, but with lower minimum values.

6.4. Future perspectives

The northwestern coast of SMG, and San Antonio Bay in particular, shows a complex dynamic. Depending on the exact location of a shell specimen or a population, environmental parameters will vary not only spatially but also seasonally (phytoplankton community structure, pigment composition, coloured dissolved organic matter, among others; Williams et al., 2013). The

shells of *A. purpurata* might hold the key to deciphering past environmental changes by studying and comparing modern and fossil specimens as well as *in situ* environmental conditions. We are confident that based on the findings of this study, *A. purpurata* is a promising archive for (spatial and temporal) environmental reconstructions. Future studies must consider a higher number of specimens and in particular more stable isotope analyses ($\delta^{18}O_{shell}$) in modern shells from different microenvironments within SMG. Also, evaporation might be an effect that needs to be taken into account in future studies. However, more evaporation in summer would lead to more positive $\delta^{18}O_{shell}$ values and therefore colder reconstructed temperatures, which is not what we see in our modern shell. Also, in the fossil shells (Pleistocene and Holocene) we can identify the summer rings (dark rings seen in thin- and cross-sections of the shell) and even those recorded warmer temperatures. A more detailed look into the stable isotope analyses in Holocene shells will then be needed in order to distinguish if environmental changes are more likely to occur due to local variations or global climate changes and which time scale these changes occur. Some environmental events during the Late Holocene, such as temperature variability, were reported for Patagonia: Neoglacial pulses, the Medieval Warm Period and the Little Ice Age (Schäbitz, 1994; Villalba, 1994; Iriondo and García, 1993; Cioccale, 1999; Prevosti et al., 2004; Meyer and Wagner, 2008; Boretto et al., 2013; Strelin et al., 2014; among others). All these climatic changes registered by different archives (pollen, tree-rings, glacial records, aeolian deposits, fossil soils, biogeographic records, etc.) were interpreted as variations in temperature, humidity as well as rainfall frequency.

7. Conclusions

We analysed a total of eleven *A. purpurata* shells from San Matías Gulf (SMG) for their potential as a new palaeoenvironmental archive for the Southern Hemisphere. All shells have been dated (AMS, LSS and ESR) demonstrating that they cover the range from the Late Pleistocene to today. Before applying any oxygen isotope analysis ($\delta^{18}O_{shell}$) all shells were checked for diagenetic alterations using CRM prior to oxygen isotope analysis.

- Shells from all epochs (Late Pleistocene, Late Holocene and modern) show similar cyclic annual $\delta^{18}O_{shell}$ patterns, which are caused by varying seasonal environmental conditions.
- Oxygen isotope values from *in situ* water samples ($\delta^{18}O_{water}$) allowed us to perform a calibration of the *A. purpurata* archive (comparison to the modern specimen) and the first careful reconstruction of palaeotemperatures, based on fossil *A. purpurata* shells, for the SMG.
- The modern shell calibration showed similar temperature values to not than the *in situ* water temperature measurements. The interpretation of palaeotemperatures is still challenging but could be highly improved in future studies by looking at more shell specimens for one particular time interval (i.e., enabling the reproducibility of results and values).

Based on these findings, we propose that *A. purpurata* offers a new palaeoarchive of past marine conditions for the northwestern coasts of Patagonia, Argentina, one that deserves more attention in future studies. However, special care must be taken with assessments based on a single specimen, especially if representing the conditions of broad time intervals within the Holocene. Observed variations may potentially reflect a variety of non/climatic differences such as microhabitats, and the complex geomorphology and water dynamics in the SMG, which themselves changed during the Holocene. Future studies with more shell specimens per time interval will help to exclude some of these uncertainties and improve our overall understanding of the region and this new palaeoarchive.

Acknowledgements

Authors want to thank Programa de Monitoreo de Calidad Ambiental de Zonas de Producción de la Provincia de Río Negro from CIMAS for providing seawater temperature data. Gernot Nehrke (AWI) is thanked for his help with the Confocal Raman microscopy. Kerstin Beyer and Lisa Schönborn (both AWI) are thanked for their help with the laboratory work related to shell preparation and stable isotope measurements at the IRMS (AWI). Financial support for this study was provided by Agencia Nacional de Promocion Cientifica y Tecnologica (ANPCyT-FONCyT)

PICT 2016-2951 awarded to S. Bayer. This study is a contribution to PUE 2016 (CICTERRA – CONICET) and to the CONICET Project (PIP 11220170100080CO).

References

Aguirre, M.L., Richiano, S., Voelker, A.H.L., Dettman, D.L., Schöne, B.R., Panarello, H.O., Donato, M., Gómez Peral, L., Castro, L.E., Medina, R., 2019. Late Quaternary nearshore molluscan patterns from Patagonia: Windows to southern southwestern Atlantic-Southern Ocean palaeoclimate and biodiversity changes? Glob. Planet. Change 181 in press. doi.org/10.1016/j.gloplacha.2019.102990

Angulo, R., Fidalgo, F., Gomez Peral, M., Schnack, E., 1978. Las ingresiones marinas Cuaternarias en la Bahía de San Antonio y sus vecindades, Prov. de Río Negro. Actas del 7° Congreso Geológico Argentino, Neuquén, p. 271-283.

Aubert, A., Lazareth, C.E., Cabioch, G., Boucher, H., Yamada, T., Iryu, Y., Farman, R., 2009. The tropical giant clam *Hippopus hippopus* shell, a new archive of environmental conditions as revealed by sclerochronological and $\delta^{18}O$ profiles. Coral Reefs 28, 989–998. doi.org/10.1007/s00338-009-0538-0

Bayer, M.S., Gordillo, S., 2013. A new Pleistocene species of *Glycymeris* (Bivalvia, Glycymerididae) from northern Patagonia, Argentina. Ameghiniana 50, 265-268.

Bayer, M.S., Gordillo, S., Morsan, E., 2014. The relictual population of the purple clam *Amiantis purpurata* (L.) in northern Patagonia (Argentina): the history of a warm-temperate-water Neogene survivor. Ameghiniana 51, 333 – 343.doi.org/10.5710/AMGH.12.05.2014.2741

Beamish, R.J., McFarlane, G.A., 1983. The forgotten requirement for age validation in fisheries biology. Trans. Am. Fish. Soc. 112(6), 735–743.

Beierlein, L., Nehrke, G., Brey, T., 2015a. Confocal Raman microscopy in sclerochronology: A powerful tool to visualize environmental information in recent and fossil biogenic archives. Geochem. Geophys. Geosyst. 16(1), 325–335. doi: 10.1002/2014GC005547.

Beierlein, L., Salvigsen, O., Schöne, B.R., Mackensen, A., Brey, T., 2015b. The seasonal water temperature cycle in the Arctic Dicksonfjord (Svalbard) during the Holocene Climate Optimum derived from subfossil *Arctica islandica* shells. Holocene 25(8), 1197–1207. doi: 10.1177/0959683615580861.

Beirne, E.C., Wanamaker, A.D., Feindel, S.C., 2012. Experimental validation of environmental controls on the delta C-13 of *Arctica islandica* (ocean quahog) shell carbonate. Geochim. Cosmochim. Acta. 84, 395-409.

Black, H.D., Andrus, C.F.T., Lambert, W.J., Rick, T., Gillikin, D.P., 2017. δ^{15}N values in *Crassostrea virginica* shells provides earliest direct evidence for nitrogen loading to Chesapeake Bay. Sci. Rep. 7 (44241). doi:10.1038/srep44241.

Boretto, G.M., Gordillo, S., Cioccale, M., Colombo, F., Fucks, E., 2013. Multi-proxy evidence of Late Quaternary environmental changes in the coastal area of Puerto Lobos (northern Patagonia, Argentina). Quatern. Int. 305, 188-205. doi.org/10.1016/j.quaint.2013.02.017

Butler, P.G., Schöne, B.R., 2017. New research in the methods and applications of sclerochronology. Palaeogeogr. Palaeoclimatol. Palaeoecol. 465, 295‑299. doi:10.1016/j.palaeo.2016.11.013

Butler, P.G., Freitas, P.S., Burchell, M., Chauvaud, L., 2019. Archaeology and sclerochronology of marine bivalves. In: Goods and Services of Marine Bivalves. Springer, Cham, pp. 413‑444.

Campana, S.E., 2001. Accuracy, precision and quality control in age determination, including a review of the use and abuse of age validation methods. J. Fish. Biol. 59, 197–242.

Carcelles, A. 1944. Catálogo de moluscos marinos de Puerto Quequén. Revista Del Museo de La Plata 3, 233–309.

Carré, M., Bentaleb, I., Fontugne, M., Lavallée, D., 2005. Strong El Nino events during the early Holocene: stable isotope evidence from Peruvian sea shells. Holocene 15,42-47. doi.org/10.1191%2F0959683605h1782rp

Castellanos, Z.A., 1967. Catálogo de moluscos marinos bonaerenses. Anales de La Comisión de Investigaciones Científicas de La Provincia de Buenos Aires 8, 1–365.

Cavallotto, J.L., Violante, R.A., 2003. Late Pleistocene and Holocene transgressions in the northern Patagonian gulfs, Argentina. Continental shelves during the last glacial cycle, IGCP 464, Gdansk, 69–70.

Chauvaud, L., Lorrain, A., Dunbar, R.B., Paulet, Y-V., Thouzeau, G., Jean, F., Guarini, J-M., Mucciarone, D., 2005. Shell of the Great Scallop, *Pecten maximus*, as a high frequency archive of palaeoenvironmental changes. **Geochem. Geophys. Geosyst**. 6, 1–15. doi:10.1029/2004GC000890

Cioccale, M.A., 1999. Climatic fluctuations in the central region of Argentina in the last 1000 years. Quatern. Int. 62, 35-47. doi:10.1016/S1040-6182(99)00021-X

Codignotto, J.O., Kokot, R.R., Marcomini, S.C., 1992. Neotectonism and sea-level changes in the coastal zone of Argentina. J. Coast. Res. 8, 125–133. https://www.jstor.org/stable/4297958

Crippa, G., Angiolini, L., Bottini, C., Erba, E., Felleti, F., Frigerio, C., Hennissen, J.A.I., Leng, M.J., Petrizzo, M.R., Raffi, I., Rainer, J., Stephenson, M.H., 2016. Seasonality fluctuations recorded in fossil bivalves during the early Pleistocene: implications for climate change. Palaeogeogr. Palaeoclimatol. Palaeoecol. 446, 234-251. doi:10.1016/j.palaeo.2016.01.029

del Rio, C.J., 2000. Malacofauna de las Formaciones Paraná y Puerto Madryn (Mioceno marino, Argentina): su origen, composición y significado bioestratigráfico. Serie Correlación Geológica (INSUGEO) 14, 77–101.

del Rio, C.J. and Martínez, S., 1998. El Mioceno marino en la Argentina y en el Uruguay. In: C.J. del Rio (Ed.), Moluscos marinos de la Argentina y del Uruguay. Anales de la Academia Nacional de Ciencias Exactas, Físicas y Naturales, Monografías 15, 6–25.

del Rio, C.J., Martínez, S., Orensanz, J.M., 2010. Tertiary roots in the Recent molluscan faunas of the Southwestern Atlantic Ocean. 3rd International Paleontological Congress (London), Programme and Abstracts, p. 140.

Dettman, D.L., Lohmann, K.C., 1995. Approaches to microsampling carbonates for stable isotope and minor element analysis: Physical separation of samples on a 20 micrometer scale. J. Sediment. Res. A65, 566–569. doi:10.1306/D426813F-2B26-11D7-8648000102C1865D

Dettman, D.L., Reische, A.K., Lohmann, K.C., 1999, Controls on the stable isotope composition of seasonal growth bands in aragonitic fresh-water bivalves (unionidae). Geochim Cosmochim Ac 63(7/8), 1049–1057. doi:10.1016/S0016-7037(99)00020-4

Doldan, M.S., de Rafélis, M., Kroeck, M.A., Pascual, M.S., Morsan, E.M., 2018. Age estimation of the oyster *Ostrea puelchana* determined from the hinge internal growth pattern. Mar. Biol. 165,119 doi:10.1007/s00227-018-3375-2

Dutton, A.L., Lohmann, K.C., Zinsmeister, W.J., 2002. Stable isotope and minor element proxies for Eocene climate of Seymour Island, Antarctica. Paleoceanography 17(2), 6-13. doi:10.1016/j.palaeo.2009.06.007

Elliot, M., Welsh, K., Chilcott, C., McCulloch, M., Chappell, J., Ayling, B., 2009. Profiles of trace elements and stable isotopes derived from giant long-lived *Tridacna gigas* bivalves: Potential applications in paleoclimate studies. Palaeogeogr. Palaeoclimatol. Palaeoecol. 280, 132–142. doi:10.1016/j.palaeo.2009.06.007

Epstein, S., Buchsbaum, R., Lowenstam, H.A., Urey, H.C., 1953. Revised carbonate-water isotopic temperature scale. Bulletin of the Geological Society of America 64, 1315-1326.

Fairbanks, R.G., 1989. A 17,000-year glacio-eustatic sea level record: influence of glacial melting rates on the Younger Dryas event and deep-ocean circulation. Nature 342, 637-642.

Favier Dubois, C.M., 2009. Valores de efecto reservorio marino para los últimos 5.000 años obtenidos en concheros de la costa atlántica norpatagónica (Golfo San Matías, Argentina). Magallania 37(2), 139-147. doi:10.4067/S0718-22442009000200008

Favier Dubois, C.M., Kokot, R., 2011. Changing scenarios in the Bajo de la Quinta San Matías Gulf, Northern Patagonia, Argentina: impact of geomorphologic processes in the human use of coastal habitats. Quatern. Int. 245, 103-110. doi:10.1016/j.quaint.2011.03.051

Favier Dubois, C., Borella, F., Tykot, R., 2009. Explorando tendencias en el uso humano del espacio y los recursos en el litoral rionegrino durante el Holoceno medio y tardío. En: Salemme, M., Santiago, F., Álvarez, M., Piana, E., Vázquez, M., y Mansur, E. (Eds.), Arqueología de Patagonia: una mirada desde el último confín, Tomo II. Utopías, Ushuaia, p. 985-997.

Fernández, M., 1987. Parámetros hidrobiológicos durante un ciclo anual en la Bahía de San Antonio. Informe. Instituto Biología Marina y Pesquera "Almirante Storni".

Feruglio, E., 1950. Descripción geológica de la Patagonia. Yacimientos Petrolíferos Fiscales III. Buenos Aires, p. 74-196.

Fucks, E., Aguirre, M.L., Deschamps, C.M., 2005. Late Quaternary continental and marine sediments of northeastern Buenos Aires province (Argentina): fossil content and paleoenvironmental interpretation. J. S. Am. Earth Sc. 20, 45-56. doi:10.1016/j.jsames.2005.05.003

Fucks, E.E., Schnack, E.J., Charó, M., 2012. Aspectos geológicos y geomorfológicos del sector N del Golfo San Matías, Río Negro, Argentina. Revista de la Sociedad Geológica de España 25, 95-105. http://digital.cic.gba.gob.ar/handle/11746/5901

Gagliardini, D.A., Rivas, A.L., 2004. Environmental characteristics of San Matías Gulf obtained from LANDSAT-TM and ETM+ data. Gayana 68, 186-193. doi:10.4067/S0717-65382004000200034

Gillikin, D.P., De Ridder, F., Ulens, H., Elskens, M., Keppens, E., Baeyens, W., Dehairs, F., 2005. Assessing the reproducibility and reliability of estuarine bivalve shells (*Saxidomus giganteus*) for sea surface temperature reconstruction: implications for paleoclimate studies. Palaeogeogr. Palaeoclimatol. Palaeoecol., 228, 70–85. doi:10.1016/j.palaeo.2005.03.047

Gillikin, D.P., Dehairs, F., Lorrain, A., Steenmans, D., Baeyens, W., André, L., 2006. Barium uptake into the shells of the common mussel (*Mytilus edulis*) and the potential for estuarine paleo-chemistry reconstruction. Geochim Cosmochim Ac 70, 395–407. doi:10.1016/j.gca.2005.09.015

Goman, M., Ingram, B.L., Strom, A., 2008. Composition of stable isotopes in geoduck (*Panopea abrupta*) shells: A preliminary assessment of annual and seasonal paleoceanographic changes in the northeast Pacific. Quatern. Int. 188,117-125. doi:10.1016/j.quaint.2007.06.038

Gordillo, S., 1998. Distribución biogeografica de los moluscos Holocenos del litoral Argentino-Uruguayo. Ameghiniana 35, 163-180.

Gordillo, S., Bayer, M.S., Boretto G., Charó M., 2014. Mollusk shells as bio-geo-archives. SpringerBriefs in Earth System Sciences (South America and the Southern Hemisphere). Springer, Cham. doi.org/10.1007/978-3-319-03476-8_9

Gordillo, S., Martinelli, J., Cárdenas, J., Bayer, M.S., 2011. Testing ecological and environmental changes during the last 6000 years: A multiproxy approach based on the bivalve *Tawera gayi* from southern South America. J. Mar. 91(7), 1413-1427. doi:10.1017/S0025315410002183

Gordillo, S., Brey, T., Beyer, K., Lomovasky, B.J., 2015. Climatic and environmental changes during the middle to Late Holocene in southern South America: A sclerochronological approach using the bivalve *Retrotapes exalbidus* (Dillwyn) from the Beagle Channel. Quatern. Int., 377, 83-90. doi:10.1016/j.quaint.2014.12.036

Gröcke, D.R., Gillikin, D.P., 2008. Advances in mollusc sclerochronology and sclerochemistry: tools for understanding climate and environment. Geo-Mar Lett. 28, 265–268. doi.org/10.1007/s00367-008-0108-4

Grossman, E.L., Ku, T.L., 1986. Oxygen and carbon isotope fractionation in biogenic aragonite: temperature effects. Chem. Geol. (Isotope Geoscience Section) 59, 59–74.

Hickson, J.A., Johnson, A.L., Heaton, T.H., Balson, P.S., 1999. The shell of the Queen Scallop *Aequipecten opercularis* (L.) as a promising tool for palaeoenvironmental reconstruction: evidence and reasons for equilibrium stable-isotope incorporation. Palaeogeogr. Palaeoclimatol. Palaeoecol. 154 (4), 325–337. doi:10.1016/S0031-0182(99)00120-0

Hippler, D., Witbaard, R., van Aken, H.M., Buhl, D., Immenhauser, A., 2013. Exploring the calcium isotope signature of *Arctica islandica* as an environmental proxy using laboratory- and

field-cultured specimens. Palaeogeogr. Palaeoclimatol. Palaeoecol. 373, 75–87. doi:10.1016/j.palaeo.2011.11.015

Iriondo, M.H., Garcia, N.O., 1993. Climatic variations in the Argentine plains during the last 18,000 years. Palaeogeogr. Palaeoclimatol. Palaeoecol. 101, 209-220. doi:10.1016/0031-0182(93)90013-9

Isla, F.I., 2013. The flooding of the San Matías Gulf: The Northern Patagonia sea-level curve. Geomorphology 203, 60-65. doi:10.1016/j.geomorph.2013.02.013

Klein, R.T., Lohmann, K.C., Thayer, C.W., 1996. Sr/Ca and 13C/12C ratios in skeletal calcite of *Mytilus trossulus*: Covariation with metabolic rate, salinity, and carbon isotopic composition of seawater. Geochim. Cosmochim. Ac. 60 (21), 4207-4221. doi:10.1016/S0016-7037(96)00232-3

Krepper, C.M., Bianchi, A., 1982. Balance calórico del mar epicontinental argentino. Acta Oceanográfica Argentina 3, 119-134.

Lanfredi, N.W., Pousa, J.L., 1988. Mediciones de corrientes, San Antonio Oeste, Provincia de Río Negro. Informe Inédito, Instituto de Biología Marina y Pesquera Almirante Storni, 13 p.

LeGrande, A.N., Schmidt, G.A., 2006. Global gridded data set of the oxygen isotopic composition in seawater. Geophys. Res. 33, L12604, doi:10.1029/2006GL026011.

Lucas, A.J., Guerrero, R.A., Mianzán, H.W., Acha, E.M., Lasta, C.A., 2005. Coastal oceanographic regimes of the Northern Argentine Continental Shelf (34-43°S). Estuar. Coast. Shelf. S. 65, 405-420. doi:10.1016/j.ecss.2005.06.015

Martínez, H., Nañes, C., Lizuain, A., Dal Molin, C., Turel, A., 2001. Hoja geológica 4166-II San Antonio Oeste. Provincia de Río Negro. *SEGEMAR* 32 p.

Martínez, S., del Rio, C., 2005. Las ingresiones marinas del Neógeno en el sur de Entre Ríos (Argentina) y Litoral Oeste de Uruguay y su contenido malacológico. Miscelánea (INSUGEO) 14, 13–26. http://www.insugeo.org.ar/libros/misc_14/pdf/01.pdf

McConnaughey, T.A., Gillikin, D.P., 2008. Carbon isotopes in mollusc shell carbonates. Geo-Mar. Lett. 28, 287-299.

Meyer, I., Wagner, S., 2008. The Little Ice Age in southern Patagonia: Comparison between paleoecological reconstructions and downscaled model output of a GCM simulation. *PAGES* News Special Section: Data-Model Comparison 16(2).

Morsan, E.M., 2003. Spatial analysis and abundance estimation of the southernmost population of purple clam, *Amiantis purpurata* in Patagonia (Argentina). J. Mar. 83, 4241-4251. doi:10.1017/S0025315403008294h

Morsan, E.M., 2007. Spatial pattern, harvesting and management of the artisanal fishery for purple clam (*Amiantis purpurata*) in Patagonia (Argentina). Ocean Coast. Manage. 50, 481–497. doi:10.1016/j.ocecoaman.2006.10.001

Morsan, E.M., Kroeck, M.A., 2005. Reproductive cycle of purple clam, *Amiantis purpurata* (Bivalvia: Veneridae) in northern Patagonia (Argentina). J. Mar. 85, 367-373. doi:10.1017/S002531540501129Xh

Morsan, E.M., Orensanz, J.M., 2004. Age structure and growth in an unusual population of purple clams, *Amiantis purpurata* (Lamarck 1818) (Bivalvia: Veneridae), from Argentine Patagonia. J. Shellfish Res. 23, 73-80.

Morsan, E., Zaidman, P., Ocampo-Reinaldo, M., Ciocco, N., 2010. Population structure, distribution and harvesting of southern geoduck, *Panopea abbreviata*, in San Matías Gulf (Patagonia, Argentina). Sci. Mar. 74 (4), 763–772. doi: 10.3989/scimar.2010.74n4763

NASA website http://data.giss.nasa.gov/o18data

Nehrke, G., H. Poigner, D. Wilhelms-Dick, T. Brey, D. Abele., 2012. Coexistence of three calcium carbonate polymorphs in the shell of the Antarctic clam *Laternula elliptica*, Geochem., Geophy., Geosyst. 13, Q05014, doi:10.1029/2011GC003996.

O'Neil, J.R., Clayton, R.N., Mayeda, T.K., 1969. Oxygen isotope fractionation in divalent metal carbonates. J. Chem. Phys. 31, 5547–5558. doi:10.1063/1.1671982

Oschmann, W., 2009. Sclerochronology: editorial. Int J Earth Sci (Geol Rundsch) 98, 1–2. doi:10.1007/s00531-008-0403-3

Pappalardo, M.P., Morsan, E.M., 2005. Regulación denso-dependiente del crecimiento individual de la almeja púrpura (*Amiantis purpurata*, Lamarck 1818). IBMP serie publicaciones 4, 3-20.

Piola, A., Scasso, L., 1988. Circulación en el golfo San Matías. Geoacta 15, 33–51.

Ponce, J.F., Rabassa, J., Coronato, A., Borromei, A.M., 2011. Paleogeographical evolution of the Atlantic coast of Pampa and Patagonia from the last glacial maximum to the Middle Holocene. Biol. J. Linn. Soc. 103, 363-379. doi:10.1111/j.1095-8312.2011.01653.x

Prendergast, A.L., Versteegh, E.A.A., Schone, B.R., 2017. New research on the development of high-resolution palaeoenvironmental proxies from geochemical properties of biogenic carbonates. Palaeogeogr. Palaeoclimatol. Palaeoecol. 484, 1–6. doi.org/10.1016/j.palaeo.2017.05.032

Prevosti, F.J., Bonomo, M., Tonni, E., 2004. La distribución de Chrysocyon brachyurus (Illiger, 1811) (Mammalia: Carnivora: Canidae) durante el Holoceno en la Argentina: Implicancias paleoambientales. J. Neotrop. Mammal. 11, 27–43. https://www.redalyc.org/pdf/457/45711104.pdf

Reimer, P., Bard, E., Bayliss, A., Beck, J., Blackwell, P., Ramsey, C., Buck, C. E., Cheng, H., Edwards, R. L., Friedrich, M., Grootes, P.M., Guilderson, T. P., Faflidason, H., Hajdas, I., Hatté, C., Heaton, T. J., Hoffmann, D.L., Hogg, A.G., Hughen, K.A., Kaiser, K.F., Kromer, B., Manning, S. W., Niu, M., Reimer, R. W., Richards, D. A., Scott, E. M., Southon, J. R., Staff, R. A., Turney, C. S. M., Van der Plicht, J., 2013. IntCal13 and Marine13 Radiocarbon Age Calibration Curves 0–50,000 Years cal BP. Radiocarbon, 55(4), 1869-1887. doi:10.2458/azu_js_rc.55.16947

Reynolds, D.J., Hall, I.R., Scourse, J.D., Richardson, C.A., Wanamaker, A.D., Butler, P.G., 2017. Biological and climate controls on North Atlantic marine carbon dynamics over the last millennium: insights from an absolutely dated shell-based record from North Icelandic Shelf. Global Biogeochem. Cy. 31, 1718-1735.

Rivas, A.L., 2010. Spatial and temporal variability of satellite-derived sea surface temperature in the southwestern Atlantic Ocean. Cont. Shelf Res. 30, 752–760. doi:10.1016/j.csr.2010.01.009

Rivas, A.L., Beier, E.J. ,1990. Temperature and salinity fields in the Northpatagonic Gulfs. Oceanol. Acta 13, 15-20.

Rivas, A.L., Pisoni, J.P., 2010. Identification, characteristics and seasonal evolution of surface thermal fronts in the Argentinean Continental Shelf. J. Marine Syst. 79, 134–143. doi:10.1016/j.jmarsys.2009.07.008

Rubo, S., Aguirre, M.L., Richiano, S.M., Medina, R.A., Schöne, B.R., 2018. *Leukoma antiqua* (Bivalvia) - A high-resolution marine paleoclimate archive for southern South America? Palaeogeogr. Palaeoclimatol. Palaeoecol. 505(15), 398-409. doi:10.1016/j.palaeo.2018.06.024

Rutter, N., Schnack, E., del Rio, J., Fasano, J.L., Isla, F.I., Radtke, U., 1989. Correlation and dating of Quaternary littoral zones along the Patagonian coast, Argentina. Quat. Sci. 8, 213–234. doi:10.1016/0277-3791(89)90038-3

Rutter, N., Radtke, U., Schnack, E.J., 1990. Comparison of ESR and aminoacid data in correlating and dating Quaternary shorelines along the Patagonian coast, Argentina. J. Coast. Res. 6, 391–411. https://www.jstor.org/stable/4297690

Scarabino, V., 1977. Moluscos del Golfo San Matías (Provincia de Río Negro, República Argentina). Inventario y claves para su identificación. Comunicaciones de La Sociedad Malacológica de Uruguay 4, 177–285.

Scasso, L.M., Piola, A.R., 1988. Intercambio neto de agua entre el mar y la atmósfera en el Golfo San Matías. Geoacta 15, 13-31.

Schäbitz, F., 1994. Holocene climatic variations in northern Patagonia, Argentina. Palaeogeogr. Palaeoclimatol. Palaeoecol. 109, 287-294. doi:10.1016/0031-0182(94)90180-5

Schöne, B.R., 2008. The curse of physiology—challenges and opportunities in the interpretation of geochemical data from mollusk shells. Geo-Mar Lett. 28, 269–285.

Schöne, B.R., Surge, D., 2005. Looking back over skeletal diaries − high-resolution environmental

reconstructions from accretionary hard parts of aquatic organisms. Palaeogeogr. Palaeoclimatol. Palaeoecol. 228, 1–3. doi.org/10.1016/j.palaeo.2005.03.043

Schöne, B.R., Fiebig, J., Pfeiffer, M., Gleh, R., Hickson, J., Johnson, A.L.A., Dreyer, W., Oschmann, W., 2005a. Climate records from a bivalved Methuselah (*Arctica islandica*, Mollusca; Iceland). Palaeogeogr. Palaeoclimatol. Palaeoecol. 228, 130– 148. doi:10.1016/j.palaeo.2005.03.049

Schöne, B.R., Dunca, E., Fiebig, J., Pfeiffer, M., 2005b. Mutvei's solution: An ideal agent for resolving microgrowth structures of biogenic carbonates. Palaeogeogr. Palaeoclimatol. Palaeoecol. 228, 149-166. doi:10.1016/j.palaeo.2005.03.054

Schöne, B.R., Houk, S.D., Freyre Castro, A. D., Fiebig, J., Oschmann, W., 2005c. Daily growth rates in shells of *Arctica islandica*: Assessing sub-seasonal environmental controls on a long-lived bivalve mollusk. Palaios 20; 78-92. doi:10.2110/palo.2003.p03-101

Schöne, B.R., Gillikin, D.P., 2013. Unraveling environmental histories from skeletal diaries-Advances in sclerochronology. Palaeogeogr. Palaeoclimatol. Palaeoecol. 373, 1–5. doi:10.1016/j.palaeo.2012.11.026

Schmidt, G.A., G. R. Bigg, Rohling, E.G., 1999. Global Seawater Oxygen-18 Database - v1.22 https://data.giss.nasa.gov/o18data/

Schmunk, R.B., 2017. Panoply netCDF, HDF and GRIB Data Viewer (Version 4.7): NASA Goddard Institute for Space Studies.

Servicio de Hidrografía Naval, 2013. http://www.hidro.gov.ar/

Strelin, J.A., Kaplan, M.R., Vandergoes, M.J., Denton, G.H., Schaefer, J.M., 2014. Holocene glacier history of the Lago Argentino basin, Southern Patagonian Icefield. Quat. Sci. 101, 124-145. doi: 10.1016/j.quascirev.2014.06.026

Stuiver, M., Reimer, P.J., Reimer, R.W., 2020. CALIB 7.1 [WWW program] at http://calib.org, accessed 2020-7-28

Surge, D., Lohmann, K.C, 2008. Evaluating Mg/Ca ratios as a temperature proxy in the estuarine oyster, *Crassostrea virginica*, J. Geophys. Res. 113, G02001, doi:10.1029/2007JG000623.

Urey, H.C., Lowenstam, H.A., Epstein, S., McKinney, C.R., 1951. Measurement of paleotemperatures and temperatures of the Upper Cretaceous of England, Denmark, and the southeastern United States. Bull. Geol. Soc. Am. 62, 399–416.

van Geldern, R., Barth, J.A.C., 2012. Optimization of instrument setup and post-run corrections for oxygen and hydrogen stable isotope measurements of water by isotope ratio infrared spectroscopy (IRIS). Limnol. Oceanogr. Methods 10, 1024–1036. doi: 10.4319/lom.2012.10.1024

Villalba, R., 1994. Tree-ring and glacial evidence for the Medieval Warm Epoch and the Little Ice Age in southern South America, in Hughes, M.K., Diaz, H. F. (Eds.). The Medieval Warm Period. Springer Netherlands, 342 pp.

von Leesen, G., Beierlein, L., Scarponi, D., Schöne, B.R., Brey, T., 2017. A low seasonality scenario in the Mediterranean Sea during the Calabrian (Early Pleistocene) inferred from fossil *Arctica islandica* shells. Palaeogeogr. Palaeoclimatol. Palaeoecol. 485, 706–714. doi:10.1016/j.palaeo.2017.07.027

Wanamaker, A.D., Kreutz, K.J., Borns, H.W., Introne, D.S., Feindel, S., Barber, B.J., 2006. An aquaculture-based method for calibrated bivalve isotope paleothermometry. Geochem. Geophys. Geosyst. 7, Q09011, doi:10.1029/2005GC001189.

Wanamaker, A.D., Kreutz, K.J., Wilson, T. 2008. Experimentally determined Mg/Ca and Sr/Ca ratios in juvenile bivalve calcite for *Mytilus edulis*: implications for paleotemperature reconstructions. Geo-Mar Lett., 28, 359–368. doi.org/10.1007/s00367-008-0112-8

Wanamaker, A.D., Kreutz, K.J., Schöne, B.R., Introne, D.S., 2011. Gulf of Maine shells reveal changes in seawater temperature seasonality during the Medieval Climate Anomaly and the Little Ice Age. Palaeogeogr. Palaeoclimatol. Palaeoecol. 302, 43-51.

Williams, G.N., Dogliotti, A.I., Zaidman, P., Solis, M., Narvarte, M.A., González, R.C., Esteves, J.L., Gagliardini, D.A., 2013. Assessment of remotely-sensed sea-surface temperature and chlorophyll-a concentration in San Matías Gulf (Patagonia, Argentina). Cont. Shelf Res. 52, 159–171. doi:10.1016/j.csr.2012.08.014

Yan, L., Schöne, B.R., Arkhipkin, A., 2012. *Eurhomalea exalbida* (Bivalvia): A reliable recorder of climate in southern South America? Palaeogeogr. Palaeoclimatol. Palaeoecol. 350–352, 91–100. doi:10.1016/j.palaeo.2012.06.018

List of Figures

Figure 1. Location map showing late Quaternary deposits in San Antonio Bay, San Matias Gulf (Argentina). **Triangle**, modern assemblages (1); **circle**, Holocene assemblages (2, 3, 4, 5, 6, 7); **square**, Pleistocene assemblages (8, 9, 10, 11) (see Section 4.1 and Table 1). Star points the bottom water sample (closed to Punta Villarino). SAO (San Antonio Oeste) is the main city in SMG. RP is a provincial road, RN is a national road.

Figure 2. *Amiantis purpurata* shell. A, shell exterior of *A. purpurata*. B, consecutive sampling from the outer shell layer in a cross-section of *A. purpurata*, using a 700 μm mill bit. DOG: direction of growth.

Figure 3. Different transgressive events in San Matias Gulf (SMG), especially in San Antonio Bay. Grey silhouette represents the modern coast, whitish silhouette represents a transgressive event. **A**, MIS 7 (Middle Pleistocene, >230000 yr B.P., Rutter et al., 1990). **B**, MIS 5e (late Pleistocene, 107000 – 42500 yr B.P.; Rutter et al., 1990). **C**. MIS 1 (Late Holocene, <4000 yr B.P.). Star symbol is the location of San Antonio Oeste (city, SAO) over time. Figure modified from Fucks et al. (2012).

Figure 4. Images of different study sites from San Matias Gulf. Refer to Figure 1 for exact locations. A and B, Site 10, Pleistocene MIS 5e outcrop. C and D, Site 7, Holocene outcrop. E, Site 3, Holocene beach ridge. F, Site 1 showing an articulated shell with periostracum. G, Site 1, modern beach (intertidal zone).

Figure 5. A, Raman spectrum of the shell P285 showing the characteristic peaks of aragonite at around 206 cm^{-1} (highlighted by grey bar) and 1085 cm^{-1}. B, CRM scan of the umbonal area of P285 showing the annual growth pattern. C, CRM scan of shell aragonite towards the ventral margin (below) where both layers can be seen.

Figure 6. Oxygen and carbon isotope profiles of seven *A. purpurata* shells from modern and Holocene deposits in San Matias Gulf. Filled circles correspond to oxygen isotope values. Open circles correspond to carbon isotope values. Vertical dotted lines correspond to ontogenetic years.

Figure 7. Oxygen and carbon isotope profiles of four *A. purpurata* shells from Pleistocene deposits in San Matias Gulf. Filled circles correspond to oxygen isotope values. Open circles correspond to carbon isotope values.

Figure 8. Palaeowater-temperatures estimated by the paleotemperature equation for aragonite shells (Grossman and Ku, 1986) of one modern and six Holocene specimens.

Figure 9. Bottom water temperature from the northwestern of San Matias Gulf through one year: April 2016 - April 2017. Temperature data was recorded every six hours (light grey background) and averaged per month (dark line) by a data recorder electronic device (Data Logger).

Table

Table 1. Information on the location coordinates and geological ages of the deposits of the study sites (cf., Fig. 1). Oxygen and carbon isotope data from Pleistocene, Holocene and modern shells of *A. purpurata*. ESR, Electron Spin Resonance. Ontogenetic ages for Pleistocene could not be assigned (cf., Section 4.5).

Site	Geographic coordinates	Shell code	Age (yr B.P.)	Dating method	Ontogenetic years sampled	$\delta^{18}O$ (‰)	$\delta^{13}C$ (‰)	$\Delta\delta^{18}O$ (‰)	$\Delta\delta^{13}C$ (‰)
1	40°49'26.28"S 64°49'32.52"W	M726	modern	$^{14}C_{AMS}$	4 - 5	-1.10 to +0.86	-6.34 to +1.80	1.96	0.87
2	40°49'41.64"S 64°51'12.30"W	H311	451-328	$^{14}C_{AMS}$	4	-0.45 to +1.41	+0.66 to +2.62	1.90	1.96
3	40°49´45,31"S 64°51´44,07"W	H534	959-820	$^{14}C_{AMS}$	7	-0.51 to +0.98	-1.18 to +2.35	1.49	0.73
4	40°47'0,45"S 64°50'26,1"W	H362	2286-2134	$^{14}C_{AMS}$	7 - 8	-0.63 to +1.11	+1.63 to +2.80	1.74	1.01
7	40°47'13.20"S 64°50'59.82"W	H688	2346-2092	$^{14}C_{LSS}$	7	-0.64 to +1.21	+1.19 to +2.60	1.85	1.43
6	40°49´19,18"S 64°43´47,52"W	H438	2351-2182	$^{14}C_{AMS}$	5	-0.29 to +1.16	+1.34 to +3.19	1.45	1.23
5	40°47'45.24"S 64°52'38.64"W	H613	3844-3555	$^{14}C_{LSS}$	8 - 9	-0.34 to +0.91	+1.47 to +2.45	1.25	0.23
8	40°49'36,4"S 64°42'1,9"W	P1143	40000-27000	ESR (Rutter et al., 1990)	---	-1.99 to +0.27	-3.53 to +1.86	2.26	3.39
9	40°42'47,1"S 64°50'56,8"W	P285	42600-42403	$^{14}C_{LSS}$	---	-0.56 to +1.12	-1.27 to +1.71	1.68	0.70
10	40°48´08,67"S 65°04´19,05"W	P1204	>107000 - 91000	ESR (Rutter et al., 1990)	---	-0.93 to +0.53	-1.02 to +1.90	1.47	2.92
11	40°42'31,1"S 64°51'56,1"W	P80	>230000 - 208000	ESR (Rutter et al., 1990)	---	-0.85 to +0.99	+0.81 to +2.28	1.84	1.09

Site	Geographic coordinates	Shell code	Age (yr B.P.)	Dating method	Ontogenetic years sampled	$\delta^{18}O$ (‰)	$\delta^{13}C$ (‰)	$\Delta\delta^{18}O$ (‰)
1	40°49'26.28"S 64°49'32.52"W	M726	modern	$^{14}C_{AMS}$	4 - 5	-1.10 to +0.86	-6.34 to +1.80	1.96
2	40°49'41.64"S 64°51'12.30"W	H311	451-328	$^{14}C_{AMS}$	4	-0.49 to +1.41	+0.66 to +2.62	1.90
3	40°49´45,31"S 64°51´44,07"W	H534	959-820	$^{14}C_{AMS}$	7	-0.51 to +0.98	-1.18 to +2.35	1.49
4	40˚47'0,45"S 64˚50'26,1"W	H362	2286-2134	$^{14}C_{AMS}$	7 - 8	-0.63 to +1.11	+1.63 to +2.80	1.74
7	40°47'13.20"S 64°50'59.82"W	H688	2346-2092	$^{14}C_{LSS}$	7	-0.64 to +1.21	+1.19 to +2.60	1.85
6	40°49´19,18"S 64°43´47,52"W	H438	2351-2182	$^{14}C_{AMS}$	[illegible]	-0.29 to +1.16	+1.34 to +3.19	1.45
5	40°47'45.24"S 64°52'38.64"W	H613	3844-3555	$^{14}C_{LSS}$	8 - 9	-0.34 to +0.91	+1.47 to +2.45	1.25
8	40˚49'36,4"S 64˚42'1,9"W	P1143	40000-27000	ESR (Rutter et al., 1990)	--	-1.99 to +0.27	-3.53 to +1.86	2.26
9	40˚42'47,1"S 64˚50'56,8"W	P285	42600-42400	$^{14}C_{LSS}$	---	-0.56 to +1.12	-1.27 to +1.71	1.68
10	40°48´08,67"S 65°04´19,05"W	P1204	>107000 - 91000	ESR (Rutter et al., 1990)	---	-0.93 to +0.53	-1.02 to +1.90	1.47
11	40˚42'31,1"S 64˚51'56,1"W	P80	>230000 - 208000	ESR (Rutter et al., 1990)	---	-0.85 to +0.99	+0.81 to +2.28	1.84

Highligths

Seasonality signal is preserved within the fossil *A. purpurata* shells from SMG.

Because SMG has its own special water dynamic *in situ* $\delta_{18}O_{sw}$ value was indispensable.

Late Holocene shells showed lower mean estimated temperatures than the modern shell.

Late Pleistocene shells showed a pronounced seasonality pattern.

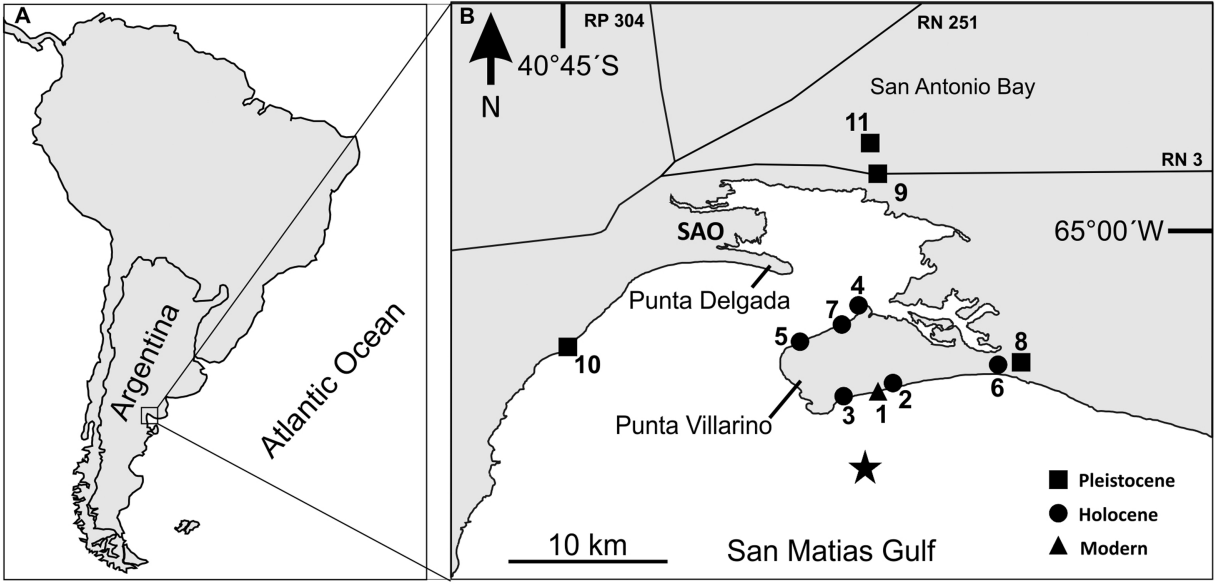
A
Argentina
Atlantic Ocean
B
RP 304
RN 251
40°45´S
N
San Antonio Bay
11
RN 3
9
SAO
65°00´W
Punta Delgada
4
7
5
8
10
6
3
1
2
Punta Villarino
Pleistocene
Holocene
Modern
10 km
San Matias Gulf

Figure 1

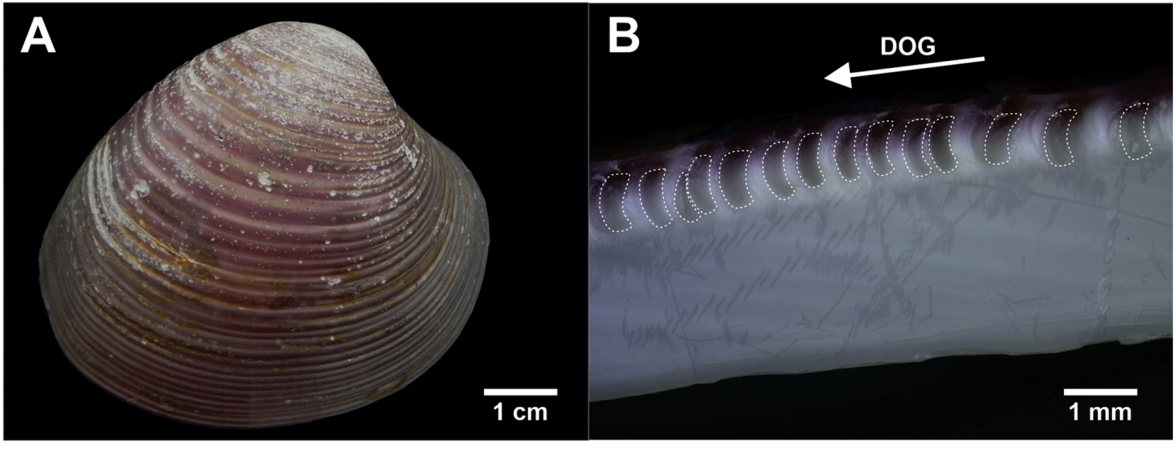

Figure 2

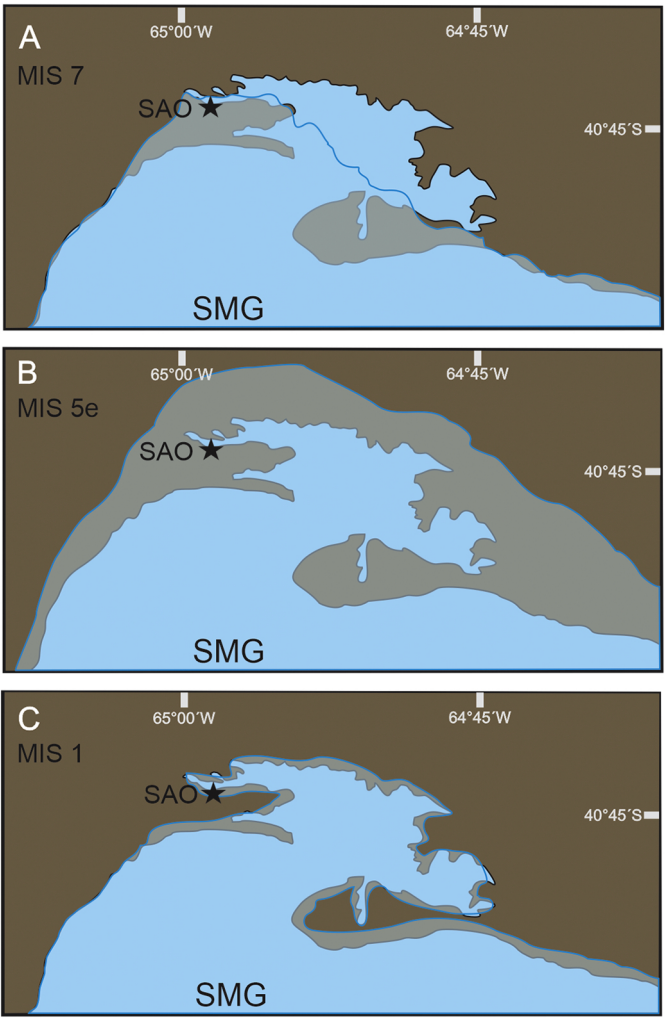
A
MIS 7
65°00´W
64°45´W
SAO
40°45´S
SMG
B
MIS 5e
65°00´W
64°45´W
SAO
40°45´S
SMG
C
MIS 1
65°00´W
64°45´W
SAO
40°45´S
SMG

Figure 3

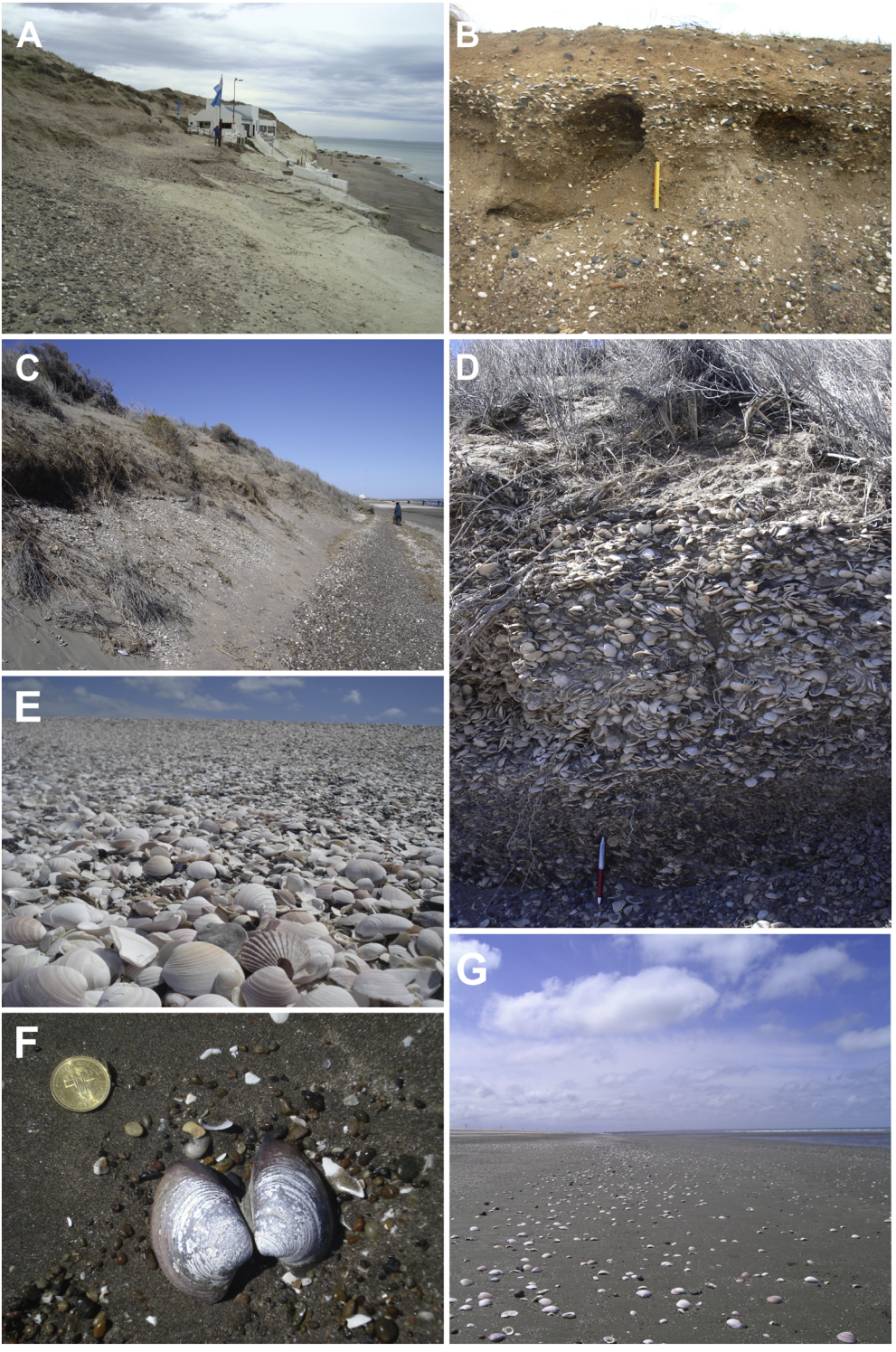

Figure 4

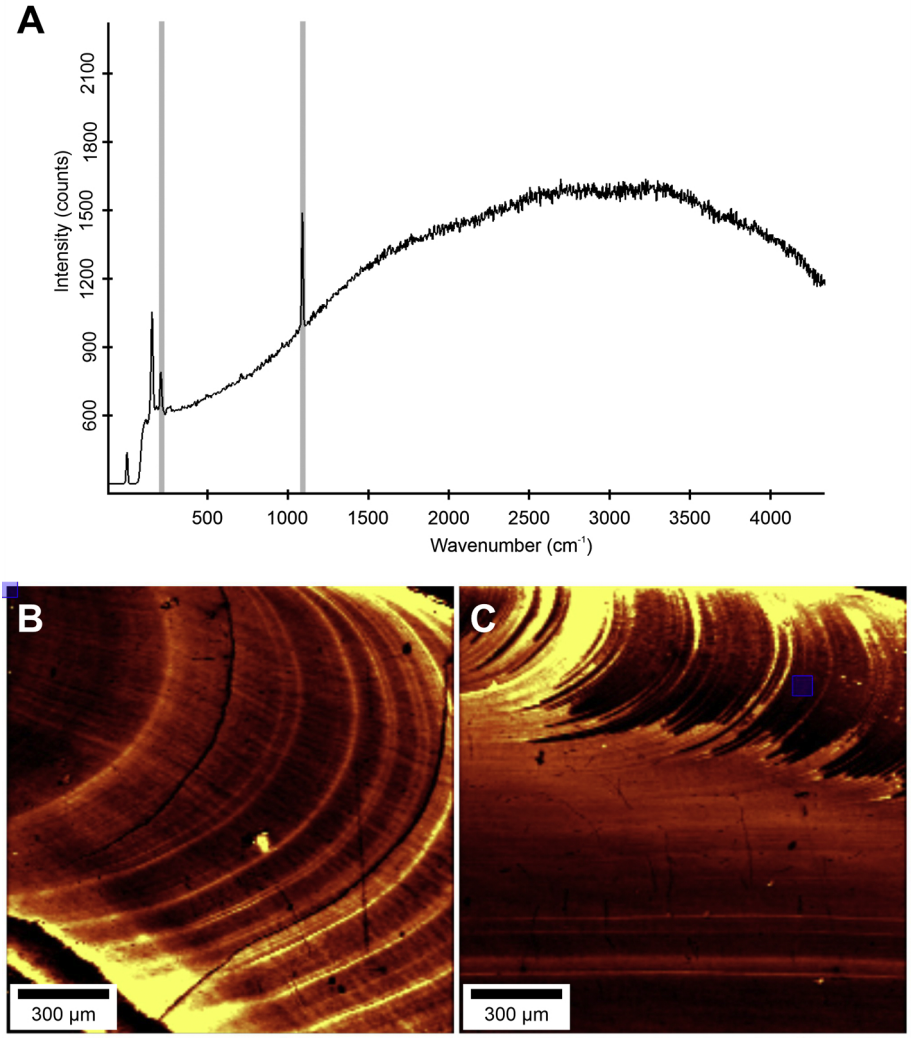
A
Intensity (counts)
600
900
1200
1500
1800
2100
500
1000
1500
2000
2500
3000
3500
4000
Wavenumber (cm-1)
B
300 µm
C
300 µm

Figure 5

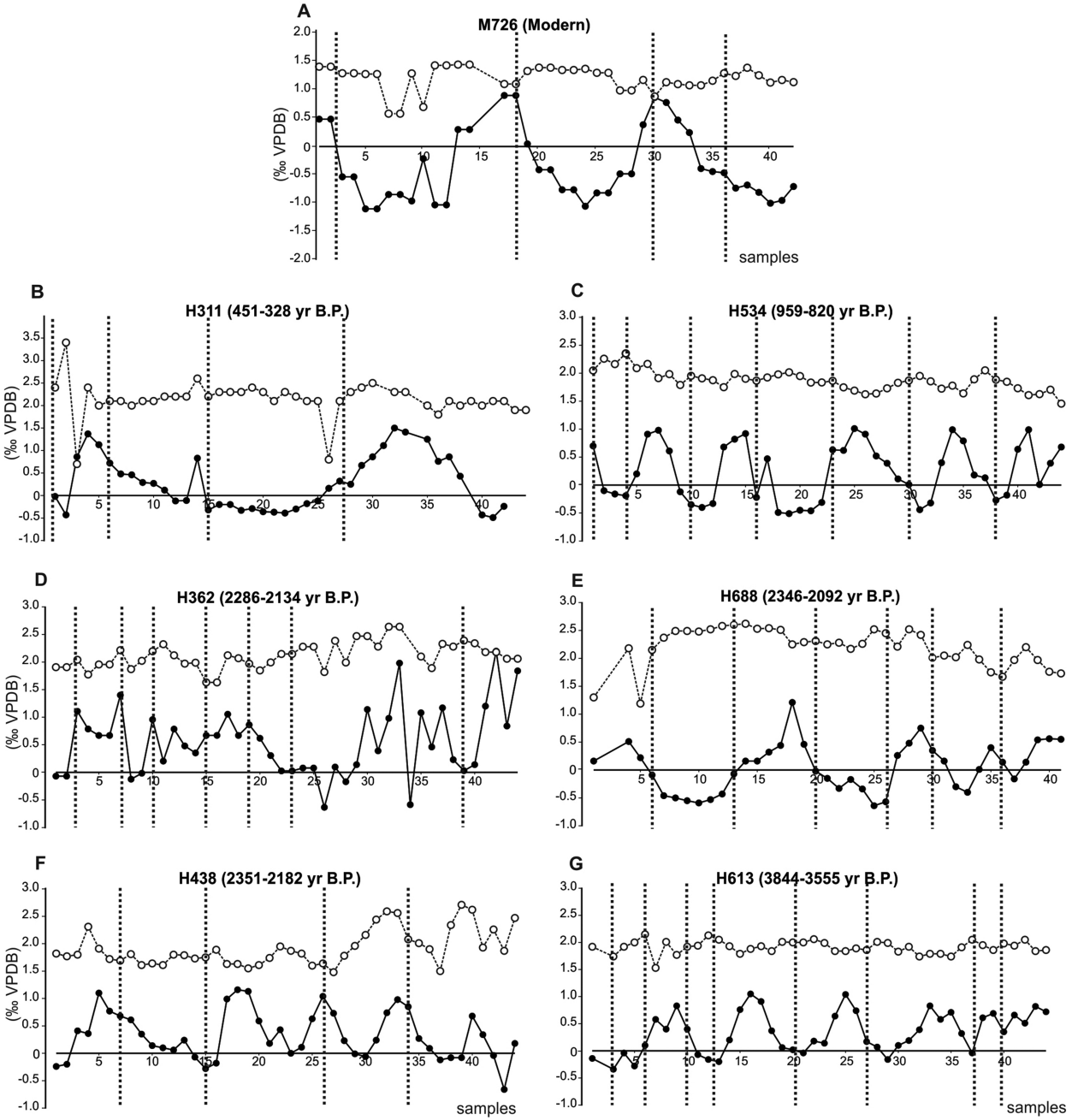
A
M726 (Modern)
(‰ VPDB)
samples
B
H311 (451-328 yr B.P.)
C
H534 (959-820 yr B.P.)
D
H362 (2286-2134 yr B.P.)
E
H688 (2346-2092 yr B.P.)
F
H438 (2351-2182 yr B.P.)
G
H613 (3844-3555 yr B.P.)

Figure 6

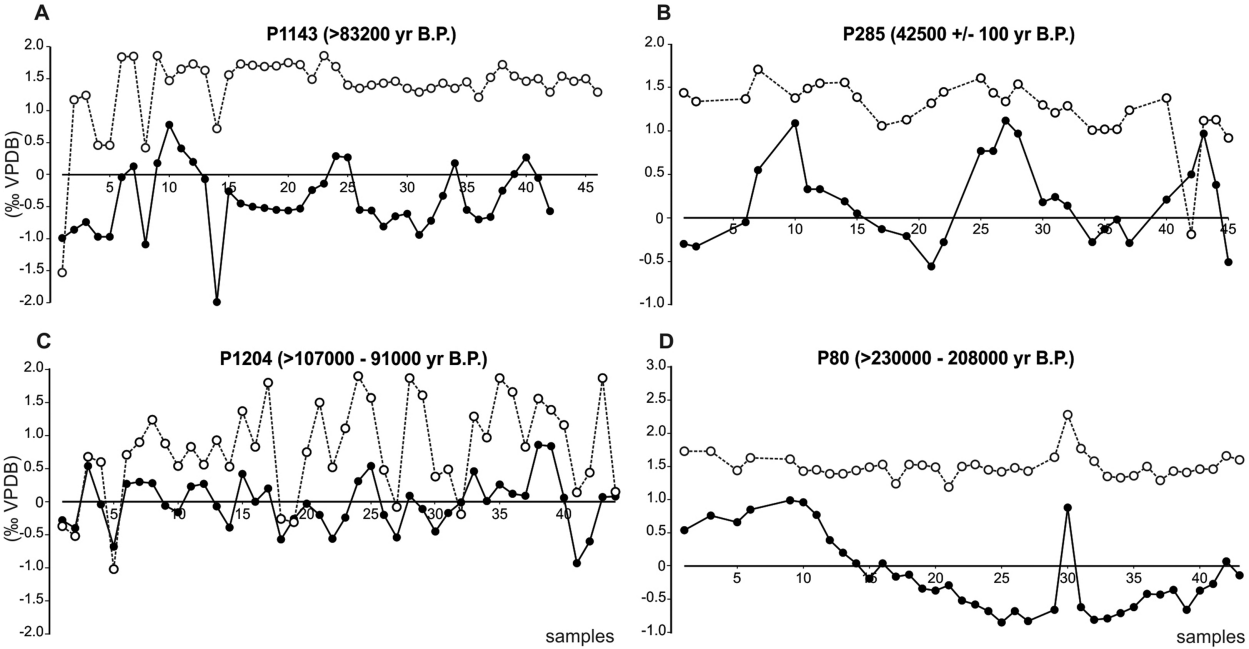
A
P1143 (>83200 yr B.P.)
(‰ VPDB)
B
P285 (42500 +/- 100 yr B.P.)
C
P1204 (>107000 - 91000 yr B.P.)
(‰ VPDB)
samples
D
P80 (>230000 - 208000 yr B.P.)
samples

Figure 7

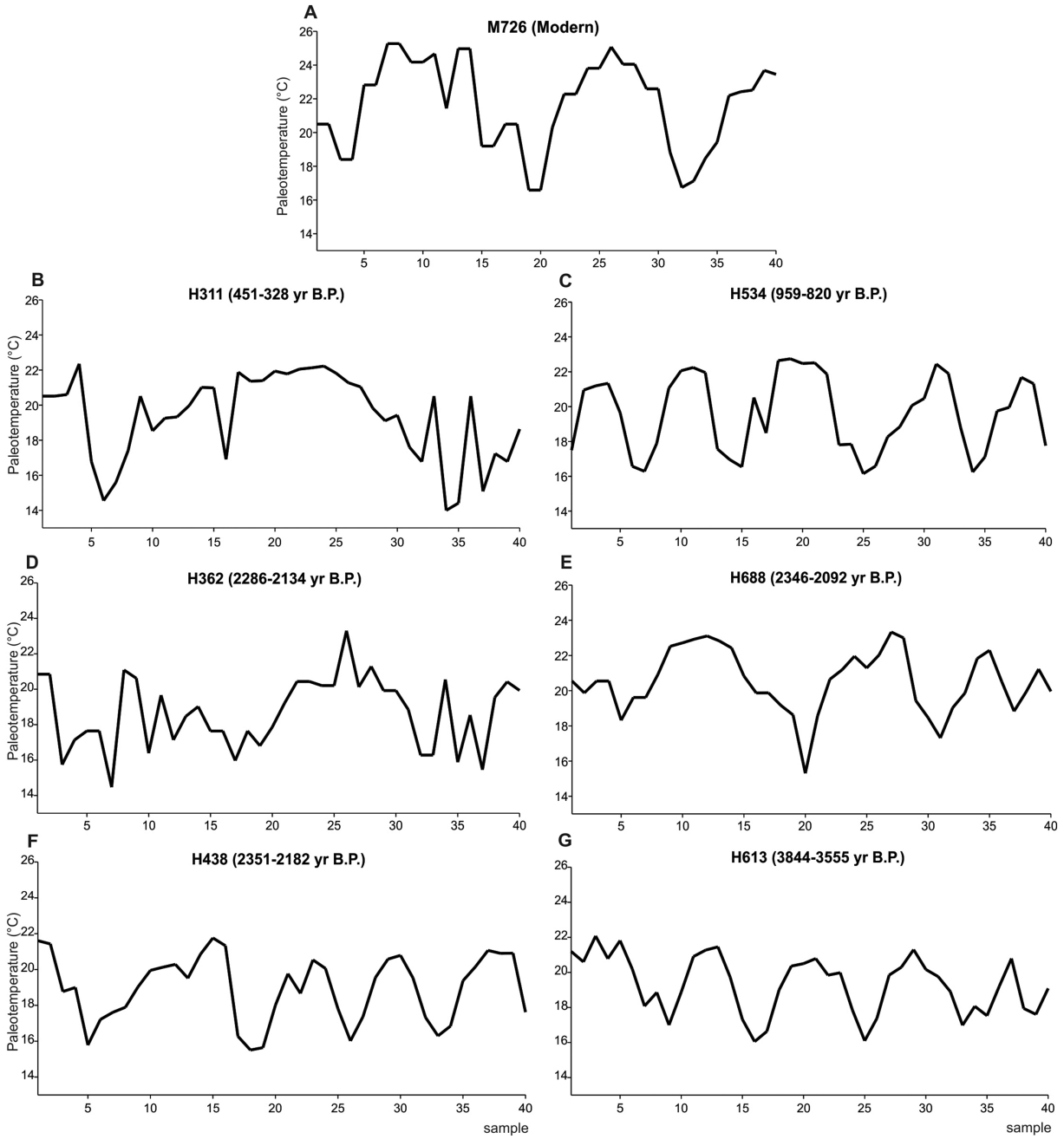
A
M726 (Modern)
B
H311 (451-328 yr B.P.)
C
H534 (959-820 yr B.P.)
D
H362 (2286-2134 yr B.P.)
E
H688 (2346-2092 yr B.P.)
F
H438 (2351-2182 yr B.P.)
G
H613 (3844-3555 yr B.P.)
Paleotemperature (°C)
sample

Figure 8

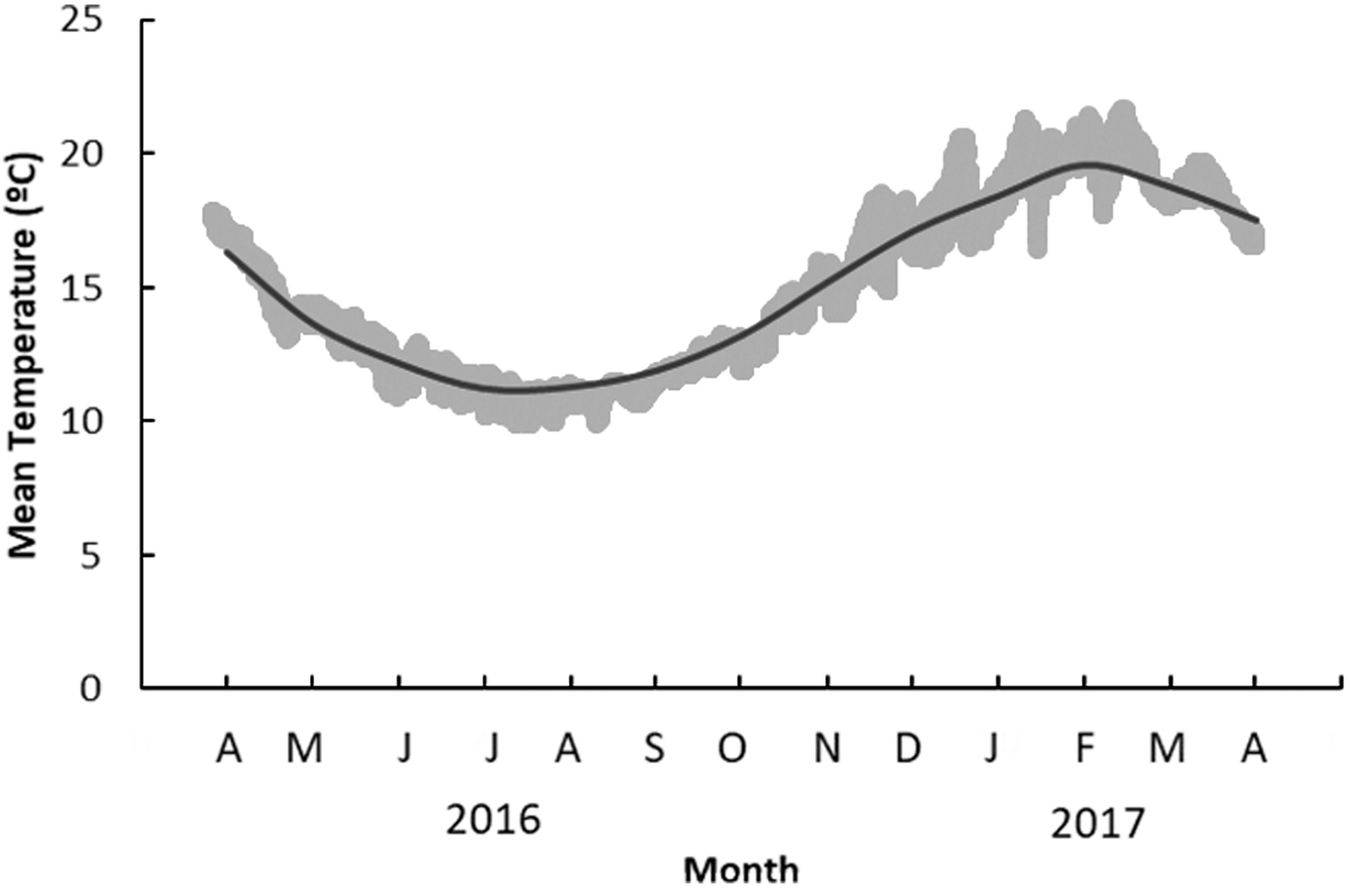
25
20
15
10
5
0
Mean Temperature (ºC)
A
M
J
J
A
S
O
N
D
J
F
M
A
2016
2017
Month

Figure 9